AN AB INITIO CALCULATION OF THE POTENTIAL ENERGY CURVES OF SOME EXCITED ELECTRONIC STATES OF OH

by

IAN WHITEMAN EASSON
B.Sc., University of British Columbia, 1969

A THESIS SUBMITTED IN PARTIAL FULFILMENT OF
THE REQUIREMENTS FOR THE DEGREE OF
MASTER OF SCIENCE

in the department
of
PHYSICS

We accept this thesis as conforming to the
required standard

THE UNIVERSITY OF BRITISH COLUMBIA
September, 1971

In presenting this thesis in partial fulfilment of the requirements for an advanced degree at the University of British Columbia, I agree that the Library shall make it freely available for reference and study. I further agree that permission for extensive copying of this thesis for scholarly purposes may be granted by the Head of my Department or by his representatives. It is understood that copying or publication of this thesis for financial gain shall not be allowed without my written permission.

Department of Physics

The University of British Columbia
Vancouver 8, Canada

Date September 28, 1971.

ABSTRACT

A series of ab initio calculations has been performed in the Born-Oppenheimer approximation for some electronic states of OH. Wavefunctions and energies are calculated variationally. The form chosen for the wavefunction is a finite linear superposition of configurations. Molecular orbitals are formed by Schmidt-orthogonalizing the atomic orbitals, each of which is represented by a single Slater-type orbital. The variational parameters are the coefficients in the linear expansion of the wavefunction, and the non-linear parameters ζ of the Slater-type orbitals.

Wavefunctions and potential energy curves are given for some of the lower-lying $^2\Sigma^-$ and $^2\Pi$ states. One result of note is that the lowest $^2\Sigma^-$ state is bound. This disagrees with an earlier calculation (Harris and Michels, 1969), but it is in accord with a recent interpretation of the spectrum (Pryce, 1971).

TABLE OF CONTENTS

LIST OF TABLES

LIST OF FIGURES

ACKNOWLEDGEMENT

I would like to thank Dr. M.H.L. Pryce, who suggested the topic, for his supervision and great patience. I would also like to thank the U.B.C. Computing Centre for the use of their facilities. Finally, I would like to thank my wife, who was as patient as Dr. Pryce and who also did the typing.

CHAPTER I

INTRODUCTION

1. Motivation

The OH molecule is one of the simpler diatomic hydrides, and has been studied experimentally for many years. Its spectrum has been detected in the upper atmosphere, in comets (Herzberg, 1971), and in the interstellar medium (Terzian and Scharlemann, 1970). Its presence in the last medium is most puzzling. It appears that the OH is forming a natural maser. Various pumping mechanisms have been proposed, none of which can satisfactorily explain all the observed features. A knowledge of the electronically excited states of OH might be helpful in selecting some possible pumping mechanisms.

Only a few electronically excited states of OH have been detected, however. The difficulty is not in the obtaining of laboratory spectra, but in their interpretation. This interpretation would be aided greatly if it were even only roughly known which bound excited states exist, how deeply bound they are, and what their equilibrium separations are.

There is a need, therefore, for a calculation from first principles of the properties of the electronically excited states of OH.

2. The Nature of Potential Energy Curves

The total non-relativistic Hamiltonian for the OH molecule is, neglecting spin,

$$H_{tot}(\vec{P}_I,\vec{R}_I,\vec{p}_i,\vec{r}_i) = \sum_{I=1}^{2} P_I^2/2M_I + \sum_{i=1}^{9} p_i^2/2m + 8e^2/|\vec{R}_1-\vec{R}_2| + \tfrac{1}{2}\sum_{\substack{i,j=1\\ i\neq j}}^{9} e^2/|\vec{r}_i-\vec{r}_j| - \sum_{I=1}^{2}\sum_{i=1}^{9} Z_I e^2/|\vec{R}_I-\vec{r}_i| \qquad (1.1)$$

In (1.1), upper-case letters refer to the nuclei, and lower-case letters to the electrons. Thus $\vec{P}_I$, M_I, Z_I are the momentum operator, mass, and charge in units of e of the I^{th} nucleus, and $\vec{p}_i$ and m are the momentum operator and mass of the i^{th} electron.

The first term in (1.1) represents the kinetic energy of the O and H nuclei. The second term is the kinetic energy of the nine electrons. The third is the repulsion between the oxygen nucleus, with charge +8e, and the hydrogen nucleus, with charge +e. The fourth is the electron-electron repulsion, and the last describes the electron-nuclei attractions.

It is desired to find some of the eigenvalues E_{tot} and eigenfunctions Ψ_{tot} of H_{tot}, to a reasonable approximation:

$$H_{tot}\,\Psi_{tot} = E_{tot}\,\Psi_{tot} \qquad (1.2)$$

To a good approximation, Ψ_{tot} can be written as the product of a part Ψ_{el} referring only to the electrons and to the relative positions of the nuclei, and a part Ψ_{nuc} referring only to the nuclei (Born and Oppenheimer, 1927). This approximation can be made plausible by the following classical argument:

The nuclei are so much more massive than the electrons that the electrons move relatively quickly. As the electrons travel around the nuclei, the nuclei hardly move at all. Thus to a good approximation, the electrons move in the field of two fixed nuclei a distance $R = |\vec{R}_1 - \vec{R}_2|$ apart. Let V(R) be the total energy of this system. Then the effect of the electrons can be simulated by the effective nucleus-nucleus potential V(R).

The problem of finding the solution of (1.2) has now been reduced in this approximation to finding the solutions of

$$H_{el}\ (\vec{p}_i, \vec{r}_i; R)\ \Psi_{el} = V(R)\ \Psi_{el} \qquad (1.3)$$

and

$$H_{nuc}(\vec{P}_I, \vec{R}_I; R)\ \Psi_{nuc} = E_{tot}\ \Psi_{nuc}, \qquad (1.4)$$

where

$$H_{el}(\vec{p}_i,\vec{r}_i;R) = \sum_{i=1}^{9} p_i^2/2m + \tfrac{1}{2} \sum_{\substack{i,j=1 \\ i\neq j}}^{9} e^2/|\vec{r}_i-\vec{r}_j|$$

$$+ 8e^2/R - \sum_{I=1}^{2} \sum_{i=1}^{9} Z_I e^2/|\vec{R}_I-\vec{r}_i| \qquad (1.5)$$

and

$$H_{nuc}(\vec{P}_I,\vec{R}_I;R) = \sum_{I=1}^{2} P_I^2/2M_I + V(R). \qquad (1.6)$$

H_{el} is the Hamiltonian for the motion of the electrons in the field of two nuclei fixed a distance R apart. Since H_{el} is invariant under translations, it depends on the positions of the nuclei only through R, considered as a fixed parameter, despite the explicit appearance of $\vec{R}_I$ in (1.5).

H_{nuc} is the Hamiltonian for the two nuclei in a potential V(R). A graph of V versus R is called a potential energy curve. There will in general be a large number of them, one for each solution of (1.3), corresponding to different electronic states.

As $R \to \infty$, potential energy curves flatten out, because the molecule separates into two non-interacting atoms or ions. As $R \to 0$, potential energy curves rise rapidly, because the term $\propto 1/R$ becomes dominant.

At intermediate values of R, potential energy curves can have any shape. One possibility is a curve which decreases monotonically as $R \rightarrow \infty$. This corresponds to a repulsive state. Another possibility is a single minimum in the curve, which, if deep enough, corresponds to a bound state. This is quite common in the lowest electronic state.

Not all curves have such a simple shape. The curve for a state of a given symmetry type* does not cross a curve of a state of the same type. Avoided curve crossing can give rise to curves of quite complicated shapes.

---

* The symmetry types are given in Chapter III.

CHAPTER II

METHOD OF CALCULATION

It is necessary to solve equation (1.3) for the energies $V^{(i)}(R)$ and the associated wavefunctions $\Psi_{el}^{(i)}$ for $i = 1,\ldots,N$, where N is the number of potential energy curves which are to be computed. The states will be labeled so that $V^{(1)}(R)$ is the lowest energy at a given R, $V^{(2)}$ is the second lowest, etc.

One of the most straightforward ways of solving (1.3) is the Variational Method. Suppose a trial wavefunction $\Psi^{(i)}$ is chosen* that depends on a finite number of parameters $\alpha_j^{(i)}(R)$. Then the values of $\alpha_j^{(i)}$ which make $\Psi^{(i)}(\alpha_j^{(i)})$ as good a solution of (1.3) as possible are those which minimize the energy.

If $V^{(i)}(R; \alpha_j^{(i)})$ is defined by

$$V^{(i)}(R; \alpha_j^{(i)}) = \frac{\int \Psi^{(i)*} H \Psi^{(i)} dV}{\int \Psi^{(i)*} \Psi^{(i)} dV} , \qquad (2.1)$$

where $\int \ldots dV$ means integration over all space, then the condition for a minimum is

$$\frac{\partial V^{(i)}(R; \alpha_j^{(i)})}{\partial \alpha_j^{(i)}} = 0 \quad ; \quad \frac{\partial^2 V^{(i)}(R; \alpha_j^{(i)})}{\partial \alpha_j^{(i)2}} > 0. \qquad (2.2)$$

---

* Henceforth, the subscript $_{el}$ on both H_{el} and Ψ_{el} will be omitted.

$V^{(i)}(R; \alpha_j^{(i)})$ is always an upper bound to the true energy $V^{(i)}(R)$.

It is convenient to divide the parameters $\alpha_j^{(i)}$ into two classes: those upon which the wavefunctions depend linearly, and those upon which they depend non-linearly. Let $\{\beta_j^{(i)}\}$, $\{\gamma_k^{(i)}\}$ be these two classes, respectively. Then the wavefunctions can be written

$$\Psi^{(i)} = \sum_j \beta_j^{(i)} \psi_j^{(i)}(\gamma_k^{(i)}) \tag{2.3}$$

For convenience, the $\psi_j^{(i)}$ are taken to be orthonormal:

$$\int \psi_j^{(i)*} \psi_k^{(i)} dV = \delta_{jk} . \tag{2.4}$$

For the next few paragraphs the internuclear distance is considered fixed at a particular value R.

If, at this R, the $\gamma_k^{(i)}$ are also fixed, it is relatively easy to calculate the $\beta_j^{(i)}$ using matrix algebra. Equation (2.2) is equivalent to the problem of finding the lowest eigenvalue $V^{(i)}(R; \alpha_j^{(i)})$ and the corresponding eigenvalue of the matrix of the electron Hamiltonian H between the basis states $\psi_j^{(i)}$.

The results still depend upon the $\gamma_k^{(i)}$. The $\gamma_k^{(i)}$ should be varied in a systematic way so that the lowest energy eigenvalue becomes a minimum.

In practice, this procedure is tedious and time-consuming, even on a high-speed computer. This is because

it must be repeated for each wavefunction $\Psi^{(i)}$ and for many values of $\gamma_k^{(i)}$ until the correct $\gamma_k^{(i)}$ are found.

One possible resolution presents itself immediately: use no non-linear parameters. If enough linear parameters are used, the set $\psi_j^{(i)}$ becomes almost complete, and no non-linear parameters are needed. A difficulty with this method is that a very large number of linear parameters are often needed to simulate the effect of a single well-chosen non-linear parameter. The approach taken in this work is to use non-linear parameters, but only as few as necessary.

Another way to speed up the calculation, although at the expense of accuracy, is to choose the $\psi_j^{(i)}$ and $\gamma_k^{(i)}$ to be independent of (i). Then the lowest eigenvalue of the H-matrix is an upper bound to $V^{(1)}(R)$, the second lowest eigenvalue is an upper bound to $V^{(2)}(R)$, etc. In this way, if the basis states $\psi_j \equiv \psi_j^{(i)}$ are well chosen, good approximations to all the desired $V^{(i)}(R)$ can be calculated with a single diagonalization of the H-matrix.

The $\beta_j^{(i)}$ are still calculated in accordance with (2.2). There is now, however, no single prescription for calculating the $\gamma_k \equiv \gamma_k^{(i)}$ since there is no longer just one eigenvalue corresponding to the set $\{\gamma_k\}$, but N of them.

One prescription often used is to choose the γ_k so that $V^{(1)}(R;\alpha_k)$ is a minimum. The lowest energy state

is then well described. It is hoped that these γ_k will also provide a reasonable description of the higher states.

If only the lowest state is to be calculated, this prescription is the best. On the other hand, if one is interested in the M lowest-lying states, where $1 < M \leq N$, there is no reason to suppose that this method will adequately describe states 2,3,...,M unless N is very large.

A different prescription is therefore used in this work. The γ_k are chosen so that the average energy of the lowest M states is a minimum. If

$$\overline{V} = 1/M \sum_{i=1}^{M} V^{(i)} \tag{2.5}$$

is the average energy, then it is required that $\overline{V}$ satisfy

$$\frac{\partial \overline{V}}{\partial \gamma_k} = 0 \quad ; \quad \frac{\partial^2 \overline{V}}{\partial \gamma_k^2} > 0 \ . \tag{2.6}$$

It is reasonable to expect that (2.6) will provide quite good γ_k, because each one of the M states of interest is thereby treated on an equal footing, in contrast with the usual prescription, which distinguishes the lowest energy state.

To produce good potential energy curves, calculations must be done at many values of R. If the above procedure had to be repeated at each R, it would be very time-consuming. It is not the calculation of the $\beta_j^{(i)}$ which is so difficult, but the determination of the γ_k. The reason

is that the only way in general to find the γ_k which minimize $\overline{V}$ is to vary γ_k systematically. For each set of trial values γ_k, the H-matrix must be calculated and diagonalized.

The solution to this difficulty adopted in this work is to calculate the $\gamma_k(R)$ at only a few selected values of R, and to estimate $\gamma_k(R)$ for other values of R by polynomial extrapolation or interpolation. The $\beta_j^{(i)}(R)$ are still calculated at all R because the calculation does not take very much time. This approach is reasonably successful because it is found that in practice the $\gamma_k(R)$ are rather smooth functions of R.

CHAPTER III

CLASSIFICATION OF THE ELECTRONIC STATES

The electronic Hamiltonian $H = H_{el}$, defined by equation (1.5), contains no spin terms. It commutes with a number of operators. These include S^2, S_z, L_z, J_z, and $\mathcal{R}$. S^2 is the square of the total spin operator, S_z is the component of spin angular momentum along the internuclear axis (z axis), L_z is the z-component of the electronic orbital angular momentum, $J_z = L_z + S_z$ is the total electronic angular momentum along the z-axis, and $\mathcal{R}$ is the operator of reflection through a plane passing through the z-axis. A number of these operators commute with each other; others do not.

For example, $\mathcal{R}$ and L_z do not commute. To see this, consider the case of one electron, rather than nine. In this case, L_z is given in co-ordinate space by

$$L_z = i \frac{\partial}{\partial \varphi} \quad , \tag{3.1}$$

where φ is the azimuthal angle in cylindrical polar co-ordinates, with the internuclear axis as the axis of symmetry. The reflection $\mathcal{R}$ in co-ordinate space causes

$$\mathcal{R} : \varphi \rightarrow -\varphi \tag{3.2}$$

and therefore

$$\mathcal{R}: \; L_z \rightarrow \mathcal{R} L_z \mathcal{R}^{-1} = -L_z \quad , \tag{3.3}$$

so $\mathcal{R}$ and L_z do not commute. In fact, $\mathcal{R}$ takes an eigenstate of L_z with eigenvalue m into an eigenstate of L_z with eigenvalue -m, as can be seen from (3.3). S_z and J_z are, like L_z, z-components of angular-momentum operators, and similar conclusions follow for them.

$\mathcal{R}$ can then be written as the product of two operators, $\mathcal{R}_L$ and $\mathcal{R}_S$, which commute with one another:

$$\mathcal{R} = \mathcal{R}_L \mathcal{R}_S = \mathcal{R}_S \mathcal{R}_L \quad . \tag{3.4}$$

$\mathcal{R}_L$ is the operator which causes

$$\mathcal{R}_L: \; L_z \rightarrow \mathcal{R}_L L_z \mathcal{R}_L^{-1} = -L_z \quad , \tag{3.5}$$

and $\mathcal{R}_S$ causes

$$\mathcal{R}_S: \; S_z \rightarrow \mathcal{R}_S S_z \mathcal{R}_S^{-1} = -S_z \quad . \tag{3.6}$$

$\mathcal{R}_L$ and $\mathcal{R}_S$ each commute with H. By (3.5), $\mathcal{R}_L$ commutes with $|L_z|$, and by (3.6), $\mathcal{R}_S$ commutes with $|S_z|$.

The operators $H, S^2, S_z, |L_z|, |J_z|$ and $\mathcal{R}_L$ then all commute with one another, and it is possible to classify the stationary states $\Psi^{(i)}$ of H into different classes labeled by the eigenvalues of $S^2, S_z, |L_z|, |J_z|$ and $\mathcal{R}_L$. The matrix elements of H between states belonging to two different classes vanish. As a result, it is only necessary to consider states of the same class when doing a calculation.

The eigenvalues of $|L_z|$ can take on the values $\hbar\Lambda$, where $\Lambda = 0,1,2$, etc. Eigenstates of $|L_z|$ with these eigenvalues are called Σ, Π, Δ, etc. states, respectively. The multiplicity of a state $\Psi^{(i)}$ is defined to be 2s+1, where

$$S^2 \Psi^{(i)} = \hbar^2 s(s+1) \Psi^{(i)} . \qquad (3.7)$$

The multiplicity is indicated by a superscript, e.g. $^2\Pi$ is a Π state with $s = \frac{1}{2}$.

Since $\mathcal{R}_L^2 = 1$, $\mathcal{R}_L$ can have eigenvalues ± 1. The appropriate eigenvalue is indicated by a superscript, e.g. $^4\Sigma^-$.

The eigenvalue of $|J_z|$, $\hbar\Omega$, is indicated by writing Ω as a subscript, e.g. $^2\Delta_{3/2}$.

Two states of different types can be degenerate. For example, the energy is independent of S_z and J_z. Also, states with $\Lambda \neq 0$ have energies which are independent of whether they have +1 or -1 as the eigenvalue of $\mathcal{R}_L$. However, if from a given Σ state which is not an eigenstate of $\mathcal{R}_L$, both a Σ^+ and a Σ^- state can be formed, then these two will not be degenerate. The explanation for this will be given in Chapter IV, Section 7, where the method of construction of $\Sigma^\pm$ states is given.

Because of this, it does not matter if the states with $\Lambda \neq 0$ are eigenvectors of $\mathcal{R}_L$. Such states can then be classified into groups labeled by the eigenvalues of

S^2,S_z,L_z, and J_z. In these groups, states which differ only in the sign of S_z,L_z, or J_z are degenerate.

Since one is interested in calculating only non-degenerate states, it will be understood in what follows that the maximum possible values of S_z and L_z are to be taken. For example, by a $^2\Pi$ state will be meant a state with $L_z = +\hbar$, $S_z = +\frac{1}{2}\hbar$.

In the next chapter, the construction of trial wavefunctions possessing symmetries such as those mentioned above will be described.

CHAPTER IV

CONSTRUCTION OF TRIAL WAVEFUNCTIONS OF A GIVEN SYMMETRY TYPE

1. Atomic Orbitals

It is well known that, to a large degree, the motions of electrons in atoms or molecules are uncorrelated, so that the electron wavefunction approximately factors into a product of one-electron wavefunctions, or orbitals.

The OH molecule has cylindrical symmetry about the internuclear axis. It is reasonable to choose orbitals which are adapted to this symmetry.

However, another approach is possible. Because the charge on the oxygen nucleus is eight times that on the hydrogen nucleus, there is, at small R, a point of rotational symmetry--the O nucleus. At large R, there is little interaction between the two nuclei, so that there are two points of spherical symmetry--the nuclei.

This suggests an alternative approach, the one taken here, namely, that the orbitals should be constructed from things which are centred on the nuclei. These atomic orbitals are of the form

$$\phi(r, \theta, \varphi) = R(r)\, Y_{lm}(\theta, \varphi). \qquad (4.1)$$

(r, θ, φ) form a spherical polar co-ordinate system, which may have its origin at either the O or H nucleus. Y_{lm} is a spherical function. This is convenient because the Y_{lm} are eigenfunctions of L_z:

$$L_z Y_{lm} = m Y_{lm} \quad . \tag{4.2}$$

Equation (4.2) is true independently of which nucleus ϕ is centred upon.

The radial part R(r) of the atomic orbital has been chosen in this work to be of the Slater form

$$R(r) = N(n, \xi) r^{n-1} e^{-\xi r} . \tag{4.3}$$

N is a normalization constant. n plays a role analogous to that of the principal quantum number in the hydrogen atom wavefunction. ξ is a parameter which determines how quickly R(r) drops off with increasing r. The ξ of the different atomic orbitals are the non-linear parameters mentioned in Chapter II. n could also have been chosen as a non-linear parameter, but this was not done for two reasons. First, one non-linear parameter per atomic orbital is probably enough. Second, if n is fixed at an integer value, the integrals which have to be evaluated are easier to calculate.

In order to provide a reasonable description of the low-lying electronic states of OH, it was decided to select atomic orbitals of two types. The first type consisted of those atomic orbitals which are occupied in the ground

states of oxygen and hydrogen. These are the 1s, 2s, and 2p orbitals on oxygen and 1s on hydrogen.

The second type consisted of those atomic orbitals not included in the first type which are occupied in the lower-lying excited states of oxygen and hydrogen. These are the 3s, 3p, and 3d atomic orbitals on oxygen and the 2s and 2p atomic orbitals on hydrogen.

The number of σ (m=0) orbitals is then nine: 1s, $2s, 2p\sigma, 3s, 3p\sigma, 3d\sigma$ on oxygen, and $(1s)_H, (2s)_H, (2p\sigma)_H$ on hydrogen. There are four π (m=+1) orbitals: $2p\pi, 3p\pi$, $3d\pi$ on oxygen, and $(2p\pi)_H$ on hydrogen. There are four corresponding $\tilde{\pi}$ (m=-1) orbitals. There is one δ(m=2) orbital: $3d\delta$ on oxygen, and a $3d\tilde{\delta}$ on oxygen. This is a total of nineteen atomic orbitals.

2. Molecular Orbitals

The atomic orbitals are not all orthogonal. For example, the overlap integral between the 2p atomic orbital and the $(1s)_H$ does not vanish, unless R=0 or R=∞.

The expressions for the matrix elements of H* are simpler if the electron orbitals are orthonormal. Orthonormal orbitals can be formed by taking appropriate linear combinations of atomic orbitals. Since these linear combinations can involve atomic orbitals centred on both

---

* See Chapter V, Section 1 for these expressions. Also see Appendix 1.

nuclei, the linear combinations may be appropriately called molecular orbitals.

There are infinitely many ways of forming orthonormal molecular orbitals from a given set of atomic orbitals, if there is one way. This can be seen as follows: One set of orthonormal molecular orbitals forms an orthonormal basis of the vector space of electron orbitals spanned by the atomic orbitals. Such a basis can be rotated at will to form another orthonormal basis, that is, another set of orthonormal molecular orbitals.

Since there is a high degree of arbitrariness in the molecular orbitals, there is freedom to choose them so that they are good approximations to the orbitals in OH. One of the convenient properties of OH is that the charge on the H nucleus is eight times smaller than that on the O nucleus. This implies that, unless OH is in a highly excited state, the inner electron orbitals are oxygen atomic orbitals. At large R, another group of molecular orbitals looks like atomic orbitals on hydrogen. The molecular orbitals formed should then be chosen so that they look as much as possible like atomic orbitals.

A way of ensuring this, which is also computationally convenient, is Schmidt orthogonalization. This procedure will be demonstrated using the σ molecular orbitals.

The innermost orbital looks much like a 1s atomic orbital on oxygen, so the first σ molecular orbital, 1σ, is chosen to be this atomic orbital:

$$1\sigma = 1s \tag{4.4}$$

The next innermost orbital looks like a 2s orbital centred on oxygen. The second σ molecular orbital, 2σ, which is chosen to represent this, consists of a 2s oxygen orbital minus enough of a 1s oxygen orbital to make 2σ and 1σ orthogonal:

$$2\sigma = \frac{2s - 1\sigma \int 1\sigma^{*}_{2s} dV}{\sqrt{\int \left(2s - 1\sigma \int 1\sigma^{*}_{2s} dV\right)^{*} \left(2s - 1\sigma \int 1\sigma^{*}_{2s} dV\right) dV}} \tag{4.5}$$

The factor $1/\sqrt{\cdots}$ ensures that 2σ is properly normalized.

The next σ molecular orbital, 3σ, consists solely of a $2p\sigma$ atomic orbital on oxygen, because the p orbital is already orthogonal to the 1σ and 2σ molecular orbitals, which are s orbitals.

The first σ molecular orbital to deserve the adjective 'molecular' because it is a linear combination of an atomic orbital on hydrogen and atomic orbitals on oxygen is the 7σ molecular orbital.

A list of the molecular orbitals and their constituents is contained in Table 4.1 on page 20.

Table 4.1

Molecular Orbitals

σ Molecular Orbitals

	Main Constituent	Other Constituents
1σ	1s	
2σ	2s	1s
3σ	$2p\sigma$	
4σ	3s	1s,2s
5σ	$3p\sigma$	$2p\sigma$
6σ	$3d\sigma$	
7σ	$(1s)_H$	$1s,2s,2p\sigma,3s,3p\sigma,3d\sigma$.
8σ	$(2s)_H$	$1s,2s,2p\sigma,3s,3p\sigma,3d\sigma,(1s)_H$
9σ	$(2p\sigma)_H$	$1s,2s,2p\sigma,3s,3p\sigma,3d\sigma$,

π Molecular Orbitals

	Main Constituent	Other Constituents
1π	$2p\pi$	
2π	$3p\pi$	$2p\pi$
3π	$3d\pi$	
4π	$(2p\pi)_H$	$2p\pi,3p\pi,3d\pi$.

δ Molecular Orbital

$1\delta = 3d\delta$.

3. Spin Eigenfunctions

By the Pauli Principle, a molecular orbital can be occupied by at most two electrons, and, if the orbital is doubly occupied, the spins of the two electrons must be antiparallel and coupled in such a way as to form a system of total spin zero. In a discussion of the spin properties of OH, then, any doubly-occupied molecular orbital can be neglected.

Since OH has nine electrons, there can be either 1, 3, 5, 7, or 9 singly-occupied molecular orbitals in the wavefunction*. The spins of the electrons in these orbitals must be such that the total wavefunction is an eigenstate of S^2 and S_z. The task at hand is then to construct spin eigenfunctions of S^2 and S_z for a given odd number of electrons.

Attention will be restricted to spin doublets ($s = \frac{1}{2}$). The reasons for this choice are explained in Chapters VII and VIII.

With one electron, there is only one way to form a state with $s = \frac{1}{2}$, $s_z = +\frac{1}{2}\hbar$, namely, spin 'up', denoted α or $\uparrow$.

With three electrons, there are two ways to form a spin doublet. The reason is seen most easily using

---

* Remember that it is assumed that the wavefunction factors into a product of molecular orbitals.

the Branching Diagrams in Figure 4.1. This type of diagram shows graphically how the spins of a group of electrons can be coupled, one at a time.

Two of the three electrons can be coupled to form either a singlet or a triplet. The singlet is shown in III-1, the triplet in III-2.

To develop explicit expressions for these states, Clebsch-Gordon coefficients are used. Let $|s,s_z;N\rangle$ denote an N-electron state which is an eigenstate of S^2 and S_z with eigenvalues $\hbar^2 s(s+1)$ and $\hbar s_z$, respectively. Then $\alpha = |\frac{1}{2},\frac{1}{2};1\rangle$ and $\beta = |\frac{1}{2},-\frac{1}{2};1\rangle$.

The singlet is

$$\begin{aligned} |0,0;2\rangle &= \sqrt{\tfrac{1}{2}}\,|\tfrac{1}{2},\tfrac{1}{2};1\rangle\,|\tfrac{1}{2},-\tfrac{1}{2};1\rangle - \sqrt{\tfrac{1}{2}}\,|\tfrac{1}{2},-\tfrac{1}{2};1\rangle\,|\tfrac{1}{2},\tfrac{1}{2};1\rangle \\ &= \sqrt{\tfrac{1}{2}}(\alpha\beta-\beta\alpha). \end{aligned} \tag{4.6}$$

The triplet with $s_z = 1$ is

$$\begin{aligned} |1,1;2\rangle &= |\tfrac{1}{2},\tfrac{1}{2};1\rangle\,|\tfrac{1}{2},\tfrac{1}{2};1\rangle \\ &= \alpha\alpha . \end{aligned} \tag{4.7}$$

The triplet with $s_z = 0$ is

$$\begin{aligned} |1,0;2\rangle &= \sqrt{\tfrac{1}{2}}\,|\tfrac{1}{2},\tfrac{1}{2};1\rangle\,|\tfrac{1}{2},-\tfrac{1}{2};1\rangle + \sqrt{\tfrac{1}{2}}\,|\tfrac{1}{2},-\tfrac{1}{2};1\rangle\,|\tfrac{1}{2},\tfrac{1}{2};1\rangle \\ &= \sqrt{\tfrac{1}{2}}(\alpha\beta+\beta\alpha). \end{aligned} \tag{4.8}$$

One electron:

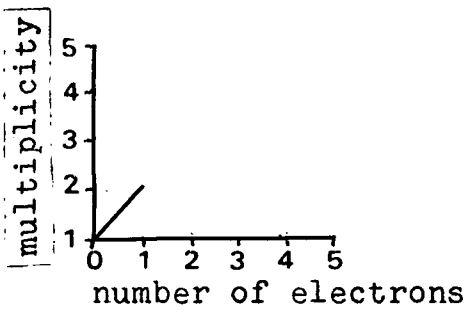

I-1

Three electrons:

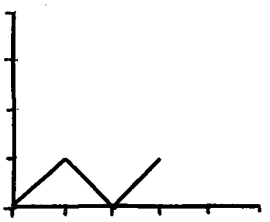

III-1

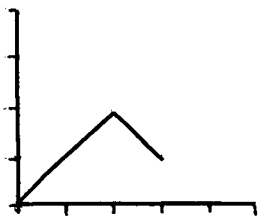

III-2

Five electrons:

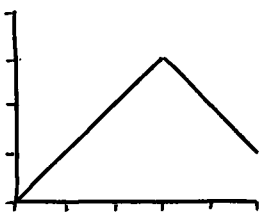

V-1

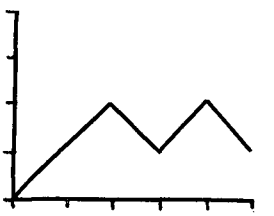

V-2

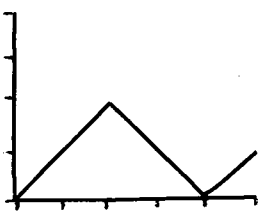

V-3

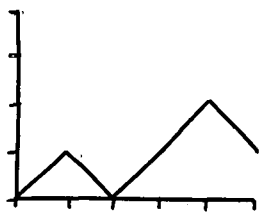

V-4

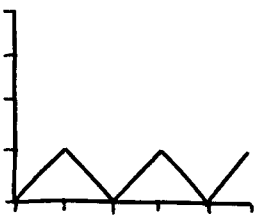

V-5

Figure 4.1. Branching Diagrams for Spin Doublets

To form a doublet with three electrons, the third electron can be coupled with either the singlet or the triplet.

If the electron is coupled with the singlet, then

$$\begin{aligned} |\tfrac{1}{2},\tfrac{1}{2};3\rangle &= |0,0;2\rangle|\tfrac{1}{2},\tfrac{1}{2};1\rangle \\ &= \sqrt{\tfrac{1}{2}}(\alpha\beta - \beta\alpha)\alpha \\ &= \sqrt{\tfrac{1}{2}}(\alpha\beta\alpha - \beta\alpha\alpha). \end{aligned} \tag{4.9}$$

If the electron is coupled with the triplet, then

$$\begin{aligned} |\tfrac{1}{2},\tfrac{1}{2};3\rangle &= \sqrt{\tfrac{2}{3}}|1,1;2\rangle|\tfrac{1}{2},-\tfrac{1}{2};1\rangle - \sqrt{\tfrac{1}{3}}|1,0;2\rangle|\tfrac{1}{2},\tfrac{1}{2};1\rangle \\ &= \sqrt{\tfrac{2}{3}}(\alpha\alpha)\beta - \sqrt{\tfrac{1}{3}}\cdot\sqrt{\tfrac{1}{2}}(\alpha\beta + \beta\alpha)\alpha \\ &= (2\alpha\alpha\beta - \alpha\beta\alpha - \beta\alpha\alpha)/\sqrt{6}\ . \end{aligned} \tag{4.10}$$

The spin states defined in (4.9) and (4.10) form an orthonormal basis of the space of eigenfunctions of S^2 and S_z corresponding to eigenvalues $\frac{3}{4}\hbar^2$ and $+\frac{1}{2}\hbar$, for three electrons. Similiar basis states can be formed for five electrons.

The basis states for one, three, and five electrons coupled to form doublets are listed in Table 4.2.

Table 4.2

Spin Eigenfunctions

One electron

I-1 : α

Three electrons

III-1 : $\sqrt{\frac{1}{2}}(\alpha\beta\alpha - \beta\alpha\alpha)$

III-2 : $(2\alpha\alpha\beta - \alpha\beta\alpha - \beta\alpha\alpha)/\sqrt{6}$

Five electrons

V-1 : $\sqrt{\frac{1}{2}}\,\alpha\alpha\alpha\beta\beta - \sqrt{\frac{1}{16}}(\alpha\alpha\beta\alpha\beta + \alpha\beta\alpha\alpha\beta + \beta\alpha\alpha\alpha\beta$
$+ \alpha\alpha\beta\beta\alpha + \alpha\beta\alpha\beta\alpha + \beta\alpha\alpha\beta\alpha$
$- \alpha\beta\beta\alpha\alpha - \beta\alpha\beta\alpha\alpha - \beta\beta\alpha\alpha\alpha)$

V-2 : $\frac{2}{3}\,\alpha\alpha\beta\alpha\beta - \frac{1}{3}\alpha\beta\alpha\alpha\beta - \frac{1}{3}\beta\alpha\alpha\alpha\beta$
$-\frac{1}{3}\alpha\alpha\beta\beta\alpha + \frac{1}{6}\alpha\beta\alpha\beta\alpha + \frac{1}{6}\beta\alpha\alpha\beta\alpha$
$-\frac{1}{6}\alpha\beta\beta\alpha\alpha - \frac{1}{6}\beta\alpha\beta\alpha\alpha + \frac{1}{3}\beta\beta\alpha\alpha\alpha$

V-3 : $\sqrt{\frac{1}{3}}(\alpha\beta\alpha\alpha\beta - \beta\alpha\alpha\alpha\beta)$
$- \sqrt{\frac{1}{12}}(\alpha\beta\alpha\beta\alpha - \beta\alpha\alpha\beta\alpha + \alpha\beta\beta\alpha\alpha - \beta\alpha\beta\alpha\alpha)$

V-4 : $\sqrt{\frac{1}{3}}(\alpha\alpha\beta\beta\alpha + \beta\beta\alpha\alpha\alpha)$
$- \sqrt{\frac{1}{12}}(\alpha\beta\alpha\beta\alpha + \beta\alpha\alpha\beta\alpha + \alpha\beta\beta\alpha\alpha + \beta\alpha\beta\alpha\alpha)$

V-5 : $\frac{1}{2}(\alpha\beta\alpha\beta\alpha - \beta\alpha\alpha\beta\alpha - \alpha\beta\beta\alpha\alpha + \beta\alpha\beta\alpha\alpha)$

4. Spatial Parts of the Configurations

Since the electrons are to a large degree uncorrelated, the spatial part, $\tilde{\psi}_j$, of each configuration* ψ_j was chosen to be a product of nine of the molecular orbitals χ_i constructed in Section 2 of this chapter. An example of a $\tilde{\psi}_j$ is

$$(1\sigma)^2(2\sigma)^2(1\tilde{\pi})(3\sigma)^2(1\pi)^2 \qquad (4.11)$$

In (4.11), the superscript ^{2} indicates that the corresponding molecular orbital is doubly occupied.

The symmetry properties of the ψ_j place certain restrictions on the possible forms $\tilde{\psi}_j$ can have. Because the ψ_j are antisymmetric, the Pauli Principle restricts the molecular orbitals χ_i in $\tilde{\psi}_j$ to be no more than doubly-occupied. The example in (4.11) obeys this restriction.

The ψ_j are eigenfunctions of S^2. Since there is only one singly-occupied molecular orbital in (4.11), (4.11) could be used only in a calculation for spin doublets.

The projection $m_{tot}\hbar$ of the total angular momentum of $\tilde{\psi}_j$ upon the internuclear axis is the sum of the projection m of the angular momentum of each molecular orbital. Thus m_{tot} for (4.11) is 1, so (4.11) can give rise only to a $^1\Pi$ state. (4.11) is, in fact, the spatial

---

* The basis states ψ_j will henceforth be called configurations.

part of that configuration which is the main contributor to the $^2\Pi$ ground state of OH at its equilibrium separation.

Even with these restrictions there are still a large number of $\tilde{\varphi}_j$ which can be formed from the nineteen molecular orbitals. From this large number, a small subset must be chosen in order to make the calculation tractable.

With a single exception, all configurations* chosen in this work have a 'frozen core'; that is, they all contain $(1\sigma)^2(2\sigma)^2$. The reasoning behind this restriction is that these innermost four electrons are well shielded by the other five from the influence of the hydrogen nucleus. This approximation will break down only in highly excited states, which are not considered here.

The orbitals $1\sigma, 2\sigma, 3\sigma, 7\sigma, 1\pi$, and $1\tilde{\pi}$ are very important in the construction of configurations because they are low in energy, and are the most important orbitals in the ground state of OH (see (4.11), for example). It is reasonable, then, to include all configurations formed from these orbitals in the calculation.

The other molecular orbitals are higher in energy. Those configurations with one singly-occupied orbital of this type can be expected to be the main constituents of the lower-lying excited states, and all such configurations should be included in the chosen subset.

---

* One $^2\Sigma^-$ configuration chosen in this work has a singly-occupied 2σ orbital. See Section 1 of Chapter VIII for a discussion of this configuration.

The configurations with two of the higher-energy orbitals will probably be quite high in energy, and thus will not be major contributors to the states of interest, in general.

In the next three sections, the combination of $\tilde{\Psi}_j$ with the spin eigenfunctions θ_k constructed in Section 3 of this chapter to form configurations of a desired symmetry type will be described.

5. Slater Determinants

The spin eigenfunctions θ_i constructed in Section 3 of this chapter are linear combinations of products single electron spins.

$$\theta_i = \sum_j c_{ji} \Theta_j \quad , \tag{4.12}$$

where the c_{ji} are real numbers, and Θ_j is a product of an odd number of α's and β's.

The problem of combining the $\tilde{\Psi}_j$ with the θ_i will be considered in the next section. In this section, the simpler problem of combining $\tilde{\Psi}_j$ with one of Θ_k will be considered.

A Slater Determinant is an antisymmetrized product of spatial and spin wavefunctions of the form

$$S_i = \mathcal{A}(\tilde{\Psi}_j \Theta_k) \, . \tag{4.13}$$

In (4.13), each doubly-occupied orbital in $\tilde{\psi}_j$ is occupied by one electron with spin up, and one with spin down. The singly-occupied orbitals of $\tilde{\psi}_j$ have their spins assigned according to Θ_k, which has as many spins as there are singly-occupied orbitals in $\tilde{\psi}_j$. Thus, for example, the un-antisymmetrized product of (4.11) with α is

$$(1\sigma\uparrow)(1\sigma\downarrow)(2\sigma\uparrow)(2\sigma\downarrow)(1\tilde{\pi}\uparrow)(3\sigma\uparrow)(3\sigma\downarrow)(1\pi\uparrow)(1\pi\downarrow)\ . \tag{4.14}$$

The above is a wavefunction in which electron number 1 is in a 1σ orbital with spin up, number 2 is in a 1σ orbital with spin down, etc. It treats the electrons, therefore, as distinguishable particles.

Because electrons are indistinguishable fermions, their wavefunction should be totally antisymmetric. The antisymmetrization operator $\mathcal{A}$ used in (4.13) accomplishes this. The application of $\mathcal{A}$ to the wavefunction (4.14) produces a wavefunction which is a sum of 9! terms. Each term is like (4.14), except that the electron labels are permuted in such a way that the total wavefunction is antisymmetric under interchange of any two electron labels.

The Slater Determinants are eigenfunctions of $\mathcal{A}$, as well as eigenfunctions of L_z and S_z. They are not, in general, eigenfunctions of S^2, $\mathcal{R}_L$, or H.

6. Configurations for Non-Σ States

The configuration ψ_j may be written as

$$\psi_j = \mathcal{A}(\tilde{\psi}_j \theta_k) \quad , \tag{4.15}$$

where θ_k is a spin eigenfunction compatible with $\tilde{\psi}_j$. Using (4.12) and (4.13), ψ_j can be written as a linear combination of Slater Determinants:

$$\psi_j = \sum_k c_{jk} S_k \quad . \tag{4.16}$$

ψ_j is an eigenfunction of L_z, $\mathcal{A}$, S^2, and S_z. It is not, in general, an eigenfunction of $\mathcal{R}_L$ or H. For non-Σ states, it is not necessary in this approximation that they be eigenfunctions of $\mathcal{R}_L$, as noted in Chapter III.

7. Configurations for Σ States

Suppose that ψ_j is a configuration which is an eigenstate of L_z, but not an eigenstate of $\mathcal{R}_L$. Define the reflected state ψ_j^R by

$$\psi_j^R = \mathcal{R}_L \psi_j \quad . \tag{4.17}$$

From ψ_j and ψ_j^R it is possible to construct two states, ψ_j^+ and ψ_j^-, which are eigenstates of $\mathcal{R}_L$ with eigenvalues +1 and -1, respectively:

$$\psi_j^{\pm} = N^{\pm}(\psi_j \pm \psi_j^R) \quad . \tag{4.18}$$

$N^{\pm}$ are normalization constants.

$$N^{\pm} = \frac{1}{\sqrt{2 \pm 2\sigma}} \quad , \tag{4.19}$$

where σ is the overlap integral

$$\sigma = \int \psi_j^{R*} \psi_j dV \quad . \tag{4.20}$$

ψ_j and ψ_j^R are degenerate.

$$\int \psi_j^{R*} H \psi_j^R dV = \int \psi_j^* H \psi_j dV = E \quad . \tag{4.21}$$

However, ψ_j^+ and ψ_j^- do not necessarily have the same energy:

$$\int \psi_j^{+*} H \psi_j^+ dV - \int \psi_j^{-*} H \psi_j^- dV = \frac{2}{1-\sigma^2}\left[\int \psi_j^{R*} H \psi_j dV - E\sigma\right]. \tag{4.22}$$

If ψ_j is an eigenstate of L_z with non-zero eigenvalue, then the right-hand side of (4.22) vanishes, and ψ_j^+ and ψ_j^- are degenerate, as noted in Chapter III. However, if ψ_j is a Σ state, then the right-hand side of (4.22) does not necessarily vanish, and the Σ^+ and Σ^- state are not, in general, degenerate.

The $\psi_j^{\pm}$ are, like ψ_j, linear combinations of Slater Determinants.

Caution must be used in the construction of eigenstates of $\mathcal{R}_L$, because a linearly dependent set of basis vectors can result. For example, the two $^2\Sigma^-$ states constructed by combining $(1\tilde{\pi})(1\pi)(3\sigma)$ with couplings III-1 and III-2 form a linearly dependent set of states. More precisely, the $^2\Sigma^-$ state formed from $(1\tilde{\pi})(1\pi)(3\sigma)$ and coupling III-1 vanishes identically.

CHAPTER V

THE HAMILTONIAN MATRIX

Once the configurations ψ_j (or $\psi_j^{\pm}$, in the case of Σ states) have been formed, the matrix elements of the Hamiltonian can be calculated.

$$H_{ij} = \int \psi_i^* H \psi_j dV \tag{5.1}$$

By (4.16), H_{ij} can be written as a linear combination of matrix elements of H between Slater Determinants.

$$H_{ij} = \sum_k \sum_l c_{ik} c_{jl} \int S_k^* H S_l dV \tag{5.2}$$

The general form of H is a sum of zero-electron, one-electron, and two-electron operators.

$$H = h_o + \sum_i h_1^{(i)} + \tfrac{1}{2} \sum_{i \neq j} h_2^{(i,j)} \quad , \tag{5.3}$$

where

$$h_o = 8/R \quad , \tag{5.4}$$

$$h_1^{(i)} = -\tfrac{1}{2} \nabla_i^2 - 8/r_i - 1/|\vec{r}_i - \vec{R}| \quad , \tag{5.5}$$

and

$$h_2^{(i,j)} = 1/|\vec{r}_i - \vec{r}_j| \quad . \tag{5.6}$$

In (5.4) to (5.6), atomic units ($e = \hbar^2/m = 1$) have been used. The unit of length is the Bohr radius and the unit of energy is the Hartree (1 Hartree $\simeq$ 27.2 e.v.). A spherical polar co-ordinate system (r, θ, φ) centred on the oxygen nucleus has been used. The hydrogen nucleus is at (R,0,0).

The expressions for the matrix elements of sums of zero, one, and two-electron operators between Slater Determinants formed from orthonormal molecular orbitals are well known (Slater, 1960). These expressions are reproduced in Appendix 1.

These expressions involve one-electron, three-dimensional integrals of the form

$$\langle \chi_i | h_1 | \chi_j \rangle = \int \chi_i^*(1) h_1^{(1)} \chi_j(1) dv(1) \quad , \qquad (5.7)$$

and two-electron, six-dimensional integrals of the form

$$\langle \chi_i, \chi_j | h_2 | \chi_k, \chi_l \rangle =$$

$$\int\int \chi_i^*(1) \chi_j^*(2) h_2^{(1,2)} \chi_k(1) \chi_l(2) dv(1) dv(2) \quad , \qquad (5.8)$$

where the volume element is

$$dv(i) = r^2 dr \sin\theta \, d\theta \, d\varphi \quad . \qquad (5.9)$$

The molecular orbitals χ_i appearing in these integrals are, as explained in Chapter IV, Section 2, linear combinations of atomic orbitals ϕ_j.

$$\chi_i = \sum_j \Delta_{ij} \phi_j \qquad (5.10)$$

The Δ_{ij} in (5.10) are real coefficients. Thus

$$\langle \chi_i | h_1 | \chi_j \rangle = \sum_a \sum_b \Delta_{ia} \Delta_{jb} \langle \phi_a | h_1 | \phi_b \rangle \ , \qquad (5.11)$$

and

$$\langle \chi_i, \chi_j | h_2 | \chi_k, \chi_l \rangle = \sum_a \sum_b \sum_c \sum_d \Delta_{ia} \Delta_{jb} \Delta_{kc} \Delta_{ld} \times \langle \phi_a, \phi_b | h_2 | \phi_c, \phi_d \rangle \ . \qquad (5.12)$$

The integrals over Slater-type atomic orbitals in (5.11) and (5.12) can be divided into two classes: one-centre and two-centre.

One-centre integrals are those in which all the atomic orbitals involved are centred on the same nucleus. There are numerically well-behaved, analytic formulas for such integrals (Joy and Parr, 1958). These formulas are reproduced in Appendix 2.

The two-centre integrals are more difficult to calculate than the one-centre integrals. Although there are analytic formulas for the former, they are often complicated, and are sometimes numerically ill-conditioned (Harris, 1969).

The method of calculation of the two-centre integrals in this work is to expand the orbitals on one centre as an infinite sum of spherical harmonics on the other centre, and then to integrate numerically. Since this method is well-

described elsewhere (Switendick and Corbato, 1963), no further description will be given here.

CHAPTER VI

IMPLEMENTATION

Three computer programs were written to perform the work outlined in Chapters IV and V.

The first program is written in FORTRAN and in the assembly language for the IBM 360. The input to this program includes information about the number of electrons, the multiplicity, the component of total orbital angular momentum along the internuclear axis, the n, l, and m values and centres for the atomic orbitals, the spatial parts of the configurations, and, if the state is a Σ state, whether it is Σ^+ or Σ^-.

The program does symbolic manipulation. It determines which non-zero integrals over atomic orbitals have to be calculated, but does not actually calculate them itself. Rather, it assigns each of these integrals a unique identifying label. The labels for the overlap integrals are used to form the symbolic expressions for the coefficients Δ_{ij} in (5.10), each of which is then given its own label. The integrals over molecular orbitals are then expanded, as in (5.11) and (5.12), as symbolic expressions involving the Δ_{ij} labels and the labels for the integrals over atomic orbitals. Equal terms in the expansion are automatically collected together. Each integral over molecular orbitals is then given its own label.

These labels are used to form the expressions given in Appendix 1 for the matrix elements of H between each pair of Slater Determinants in the calculation. Equal terms in the expressions are collected together. Each matrix element of H between Slater Determinants is given its own label. Finally, these labels are used to form the expressions (5.2) for the matrix elements of H between each pair of configurations in the calculation. The only numerical calculation in the first program is the multiplication in (5.2) of c_{ik} by c_{jl}, which are numbers.

The output from this program is of two kinds. The first kind is a printout of all the symbolic expressions formed. This printout is very useful as a debugging tool. The second kind of output is a series of numbers which are written on a disc file. This series of numbers contains essentially the same information as the printout.

There is a great advantage in having a separate program to perform the algebra. The advantage is that the algebra is done once and for all, and the results may be used repeatedly by the second program.

The second program is written in FORTRAN alone. It reads in the output on the disc file from the first program. This output tells it what things to calculate, and in what order to calculate them.

In order to perform this calculation, several numbers must be supplied. Three of these, Z_1, Z_2, and R,

are read in. The non-linear parameters $\boldsymbol{\zeta}$ must also be supplied. They can be read in, interpolated or extrapolated, or be supplied automatically by a third program, about which more will be said presently.

Given these numbers and the instructions from the first program, the second program calculates all integrals and forms the H-matrix. The matrix is diagonalized, and its eigenvalues and eigenvectors are calculated.

The third program mentioned above is a general program to find an unconstrained minimum of a function of several variables (Powell, 1964). In this case, the variables are the $\boldsymbol{\zeta}_i$, and the function is usually the $\overline{V}$ of (2.5).

CHAPTER VII
$^2\Pi$ CALCULATION

1. Outline of Calculation

The first series of calculations in this work was for $^2\Pi$ states, because the ground state of OH is a $^2\Pi$ state (Herzberg, 1971), and little is known of any other $^2\Pi$ states (Pryce, 1971).

Listed in Table 7.1 are the spatial parts of the configurations chosen for this calculation, as well as the spin couplings. An examination of this table reveals that the guidelines for selecting $\tilde{\psi}_j$ outlined in Chapter IV, Section 4 have not been completely followed. For example, the configuration $(1\sigma)^2(2\sigma)^2(1\tilde{\pi}\uparrow)(1\pi)^2(7\sigma)^2$ was not included, as it should have been.

Furthermore, of the five possible five-electron spin couplings of Table 4.2, only one, coupling V-1, was used. The reason for this choice was Hund's rule, which suggests that a state with this coupling is lower in energy than a state with either of the other four couplings, provided the spatial parts of the states are the same.

The explanation for this failure to follow the guidelines is inexperience with the program. In fact, the guidelines were altered as more calculations were performed, and attained their present form only after the calculations reported here had been completed.

The orbital parameters ζ_i were constrained to be equal for each group of $2\ell+1$ atomic orbitals of a given n and ℓ-value, for example, for the group of three 2p orbitals on oxygen. For the two separated, non-interacting atoms, all the $2\ell+1$ ζ's within such a group are equal, by rotational symmetry. Even in the interacting case, axial symmetry dictates that the ζ's are equal for two orbitals which differ otherwise only in the sign of their m-values. It was expected, therefore, that forcing all $2\ell+1$ ζ's in a group to be equal would not be a bad approximation, particularly at moderate and large internuclear separations. A short discussion of the effectiveness of this approximation is contained in Section 2 of this chapter.

At a given R, the orbital parameters ζ_i were calculated by minimizing the trace of the Hamiltonian matrix. This is equivalent to minimizing the average energy V of all twenty-nine configurations. Only the diagonal elements of H need be computed because the trace is invariant under diagonalization. There is thus a large saving in computer time. It was hoped that the orbital parameters calculated in this manner would be good enough for the low-lying states of interest. A discussion of the effectiveness of this method is in Section 2 of this chapter.

The trace was minimized at R=1.8342, 6, 10, and 15. R=1.8342 is the equilibrium separation of the ground

state (Herzberg, 1971). R=6 and 10 were chosen because they are moderate and large internuclear distances, respectively. R=15 was chosen because it was found that not all the potential energy curves had completely flattened out near R=10.

To calculate a parameter value at other than these four points, a parabola was fitted to the closest three points, and the parameter value at the point of interest was then interpolated or extrapolated.

Graphs of the parameter values as functions of R are shown in Figures 7.1 to 7.9. With several exceptions, these are smooth functions of R. Each graph has a discontinuity at R=8, because the two parabolas fitted through (1.8342, 6, 10) and (6, 10, 15) do not give the same parameter value at $\frac{1}{2}(6+10)=8$. These discontinuities are particularly acute for the 3s, 3p, $(2s)_H$, and $(2p)_H$ atomic orbital parameters.

The discontinuities could be eliminated by fitting a single cubic rather than two parabolas. However, another approach is possible. This alternative approach is based on the observation that a parameter graph can be roughly divided into two regions. The first region, $R<6$, is the region where the O and H atoms interact considerably, with a resultant large change in orbital parameters with R. In the second region, $R>6$, there is less interaction between the two atoms, and the $\zeta(R)$ curves are much smoother.

If the best orbital parameters were calculated at a third point in the first region, halfway between 1.8 and 6, for example, then not only would the results be better in the first region, but the discontinuity in the second region would be smaller.

The calculated potential energy curves for the lower-lying $^2\Pi$ states are given in Figure 7.10. A discussion of the lowest four curves follows.

2. The Ground State

There are actually two calculated potential energy curves for the ground state of OH shown in Figure 7.10. The upper one, which will be discussed first, is the curve calculated as explained in the previous section.

This first curve is qualitatively correct. It predicts that the lowest $^2\Pi$ state is bound and separates into oxygen in its ground (^3P) state and hydrogen in its ground (^2S) state. The calculated equilibrium separation, about 2.2, is approximately 25% larger than the experimentally observed separation. The calculated binding energy, about .035 Hartrees, is considerably smaller than the experimental value of about .16 Hartrees (Carlone, 1969). The quantitative agreement with experiment is therefore poor.

The wavefunction for this state as a function of R is given in Figure 7.11. The amplitudes of all major

contributors to the wavefunction, the $\beta_j^{(1)}$ of equation (2.3), are plotted. A 'major contributor' is defined to be a configuration whose amplitude, in absolute value, exceeds .1 for some value of R.

For $R < 2.3$, the largest contributor is configuration #1, in which all nine electrons are centred on the oxygen nucleus. The next largest contributor is #19, which is similiar to #1, except that a 3σ electron on oxygen has been changed into a 7σ electron on hydrogen. In #19, the $1\tilde{\pi}$ and 3σ orbitals are coupled to form a spin triplet, which is then coupled with the 7σ to form a doublet. Configuration #18, which has the same spatial part as #19, differs in that the $1\tilde{\pi}$ and 3σ are coupled to form a singlet. Since the amplitude for #18 is about $-\frac{1}{2}$ times the amplitude for #19, the combined effect of #18 and #19 is a configuration in which the 3σ and 7σ are coupled to form a singlet, which is then coupled with the $1\tilde{\pi}$ to form a doublet. This mixes very well with #1, in which the two 3σ's are coupled to form a singlet.

The next most important configurations are those in which a 1π (or $1\tilde{\pi}$) orbital centred on oxygen in #1 is replaced by a 4π (or $4\tilde{\pi}$) orbital centred on hydrogen. These are configurations #25 and #27.

In the region of the equilibrium separation, then, the bond between O and H is a σ bond with some π-type character.

As $R \rightarrow \infty$, configuration #19 becomes predominant, and all other configurations except #3, #5, and #7 become insignificant. What is happening is that an electron which at small R is in a $2p\sigma$ orbital on oxygen attaches itself to the hydrogen and occupies a pure $(1s)_H$ orbital as $R \rightarrow \infty$. Even at R=12, though, this electron has a probability amplitude of about .1 of being in a diffuse 4σ, 5σ, or 6σ orbital centred on oxygen. As can be seen, the amplitudes for configurations #3, #5, and #7 are decreasing with increasing R at R=12, and should go to zero as $R \rightarrow \infty$.

The form of the wavefunction seems quite reasonable. Why then is the potential energy curve so poor? It could be that the orbital parameters chosen by the method of minimizing the trace of H are poor choices for the ground state.

To test this guess, a second calculation was performed for the ground state alone. The orbital parameters for the 2s, 2p, and $(1s)_H$ orbitals were chosen to minimize the lowest eigenvalue of H. The orbital parameter for the $2p\sigma$ orbital was allowed to vary independently of the $2p\pi$, $2p\tilde{\pi}$ parameter. The other orbital parameters were fixed at the values obtained by minimizing the

trace of H. This was done at both R=1.8342 and 6. At R=6 there was no change in the parameters. At R=1.8342, however, there was a large change in the $(1s)_H$ orbital, and moderately large changes in the $2p\pi$ ($\tilde{\pi}$) and $2p\sigma$ orbitals (see Figures 7.3 and 7.7). The 2p orbitals became more diffuse (ζ decreased), and the $(1s)_H$ orbital contracted considerably. As can be seen from Figure 7.12, though, the amplitudes of the major configurations changed very little.

The resulting potential energy curve is the lowest curve of Figure 7.10. The predicted equilibrium separation is about 1.8, in very good agreement with experiment. The predicted binding energy is about .1 Hartrees, in fair agreement with experiment.

Several conclusions can be made at this point. The method of minimizing the trace of the H-matrix is definitely not good enough for any more than a qualitatively correct calculation. The reason for this is probably as follows. There are a large number of configurations in the calculation which are quite unlike the ground state wavefunction. Minimizing the trace treats these configurations as if they were just as important to the ground state as those which are its major components. This is true not just for the ground state, but for all states. The method, in trying to describe all states equally well, describes each state poorly.

The constraint that all $2\ell+1$ parameters of a group be equal should be relaxed at small internuclear distances. Figure 7.3 shows that at R=1.8342, the difference between the $2p\pi$, $2p\tilde{\pi}$ parameter and the $2p\sigma$ parameter, while not very large, is not insignificant. At moderate and larger ($R \geq 6$) distances, as expected, the constraint should be retained.

There are several things which could be done to increase the calculated binding energy further. One is to include a configuration with a doubly-occupied 7σ orbital. Another is to find the best parameter values for the $[2p\pi(\tilde{\pi})]_H$ and $(2p\sigma)_H$ atomic orbitals, which are present in some important configurations near the equilibrium separation. If these things were done, the overall agreement with experiment would probably be quite good.

3. The First Excited $^2\Pi$ State

According to its calculated potential energy curve, the first electronically excited $^2\Pi$ state is unbound. Beginning about R=5, the curve rises slowly and then more rapidly as $R \rightarrow 0$. At large R, the energy separation between it and the ground state is calculated to be .10 Hartrees, in good agreement with the actual value of .08 Hartrees (Edlén, 1943).

On the basis of experience with the ground state results, it can be reasonably expected that the potential energy curve for the first excited $^2\Pi$ state is qualitatively correct; i.e., that it is actually an unbound state.

The wavefunction is given in Figure 7.13. For $R > 3$, it is very much like the wavefunction for the ground state. The important difference is that in the first excited $^2\Pi$ state, the $1\tilde{\pi}$ and 3σ orbitals are coupled, at large R, to form a singlet, whereas in the ground state they are coupled to form a triplet. This excited state dissociates into hydrogen in its ground (^2S) state and oxygen in its first excited (^1D) state.

There is an extremely abrupt change in the wavefunction at R=2.3. For $R < 2.3$, configurations in which a 2π orbital is present predominate.

4. The Second Excited $^2\Pi$ State

As can be seen from Figure 7.14, the wavefunction for the second excited $^2\Pi$ state is considerably more complicated than that of either the ground state or the first excited $^2\Pi$ state. The reason for this complexity is the avoidance of curve crossing.

For $R < 2.3$, the dominant configurations are those in which a 3π orbital is singly-occupied. For $2.3 < R < 7.6$, it is the 2π orbital which is singly-occupied. In the lower

part of this range, $2.3 < R < 3.6$, the major configuration, #9, is composed of orbitals centred on oxygen. In the upper part, $3.6 < R < 7.6$, the major configuration is #28, which is similiar to #9, except that one of the electrons in a 3σ orbital on oxygen has been changed to an electron in a 7σ orbital, concentrated near the hydrogen nucleus.

At R=7.6, there is an abrupt change in the wave-function due to avoided curve crossing. Two configurations, #23 and #21, predominate. They consist of oxygen in its ground (^3P) state and an electron in a $2p\sigma$ and 3s orbital on hydrogen, respectively. An enumeration of the combinations of states of non-interacting oxygen and hydrogen atoms which can give rise to $^2\Pi$ molecular states shows in fact that the combination with the third lowest total energy is oxygen in its ground state and hydrogen with its electron in a 2s or 2p orbital.

It is not surprising that there is a large mixture of #23 and #21, since, at large R, the $(2p\sigma)_H$ and $(2s)_H$ orbitals are degenerate. Also, it is not surprising that #23 should be somewhat more important than #21, since the $(2p\sigma)_H$ orbital has, unlike the $(2s)_H$, a lobe which lies along the internuclear axis.

The potential energy curve, shown in Figure 7.10, has two minima, one at R=2.6 and one at R=9.5, with a maximum at R=6.5. The binding energy for the minimum at R=2.6 appears to be roughly the same as for the ground state.

The vibrational levels of this state will be overlaid by the vibrational levels of the third excited state, making spectroscopic identification difficult.

The broad, shallow minimum at R=9.5 should be almost impossible to detect because there are no well-known states of OH to which a transition could be made from this minimum.

Of course, these features of the potential energy curve should not be taken too seriously, because of the poorness of this first calculation.

Table 7.1

Configurations for $^2\Pi$ Calculation

Configuration Number	Spatial Part	Spin Coupling
1	$(1\sigma)^2(2\sigma)^2(1\tilde{\pi})(3\sigma)^2(1\pi)^2$	I-1
2,3	$(1\sigma)^2(2\sigma)^2(1\tilde{\pi})(3\sigma)(1\pi)^2(4\sigma)$	III-1,2
4,5	$(1\sigma)^2(2\sigma)^2(1\tilde{\pi})(3\sigma)(1\pi)^2(5\sigma)$	III-1,2
6,7	$(1\sigma)^2(2\sigma)^2(1\tilde{\pi})(3\sigma)(1\pi)^2(6\sigma)$	III-1,2
8,9	$(1\sigma)^2(2\sigma)^2(1\tilde{\pi})(3\sigma)^2(1\pi)(2\pi)$	III-1,2
10,11	$(1\sigma)^2(2\sigma)^2(1\tilde{\pi})(3\sigma)^2(1\pi)(3\pi)$	III-1,2
12	$(1\sigma)^2(2\sigma)^2(1\tilde{\pi})^2(1\pi)^2(2\pi)$	I-1
13	$(1\sigma)^2(2\sigma)^2(1\tilde{\pi})^2(1\pi)^2(3\pi)$	I-1
14	$(1\sigma)^2(2\sigma)^2(3\sigma)^2(1\pi)^2(2\tilde{\pi})$	I-1
15	$(1\sigma)^2(2\sigma)^2(3\sigma)^2(1\pi)^2(3\tilde{\pi})$	I-1
16,17	$(1\sigma)^2(2\sigma)^2(1\tilde{\pi})^2(3\sigma)(1\pi)(1\delta)$	III-1,2
18,19	$(1\sigma)^2(2\sigma)^2(1\tilde{\pi})(3\sigma)(1\pi)^2(7\sigma)$	III-1,2
20,21	$(1\sigma)^2(2\sigma)^2(1\tilde{\pi})(3\sigma)(1\pi)^2(8\sigma)$	III-1,2
22,23	$(1\sigma)^2(2\sigma)^2(1\tilde{\pi})(3\sigma)(1\pi)^2(9\sigma)$	III-1,2
24,25	$(1\sigma)^2(2\sigma)^2(1\tilde{\pi})(3\sigma)^2(1\pi)(4\pi)$	III-1,2
26	$(1\sigma)^2(2\sigma)^2(1\tilde{\pi})^2(1\pi)^2(4\pi)$	I-1
27	$(1\sigma)^2(2\sigma)^2(3\sigma)^2(1\pi)^2(4\tilde{\pi})$	I-1
28	$(1\sigma)^2(2\sigma)^2(1\tilde{\pi})(3\sigma)(1\pi)(2\pi)(7\sigma)$	V-1
29	$(1\sigma)^2(2\sigma)^2(1\tilde{\pi})(3\sigma)(1\pi)(3\pi)(7\sigma)$	V-1

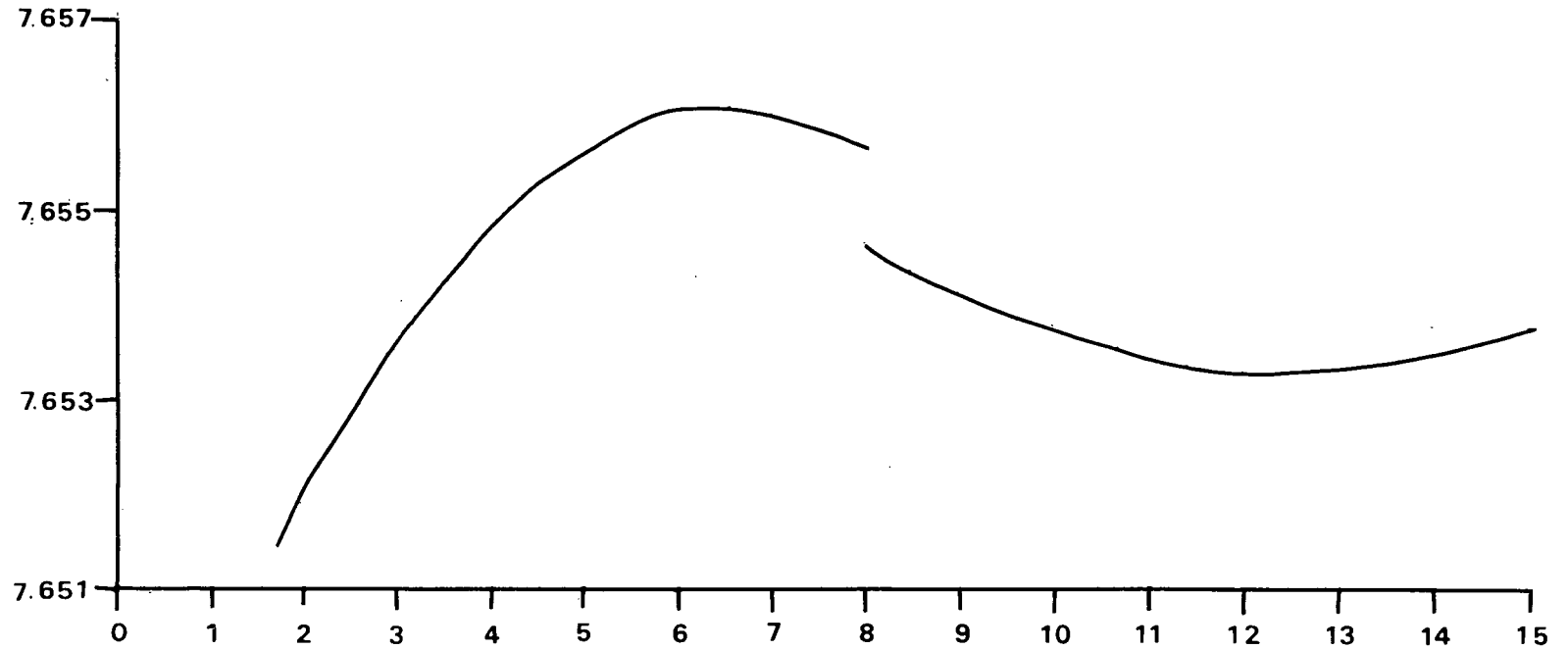

Figure 7.1. ls Parameter versus Internuclear Distance in Bohr Radii.

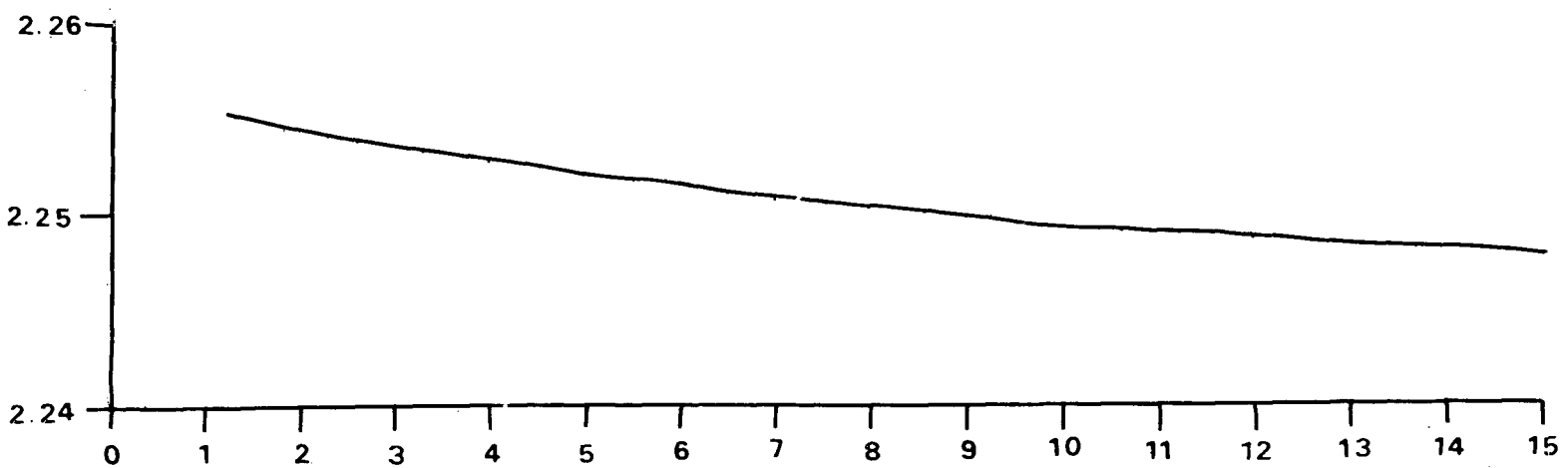

Figure 7.2. 2s Parameter versus Internuclear Distance in Bohr Radii.

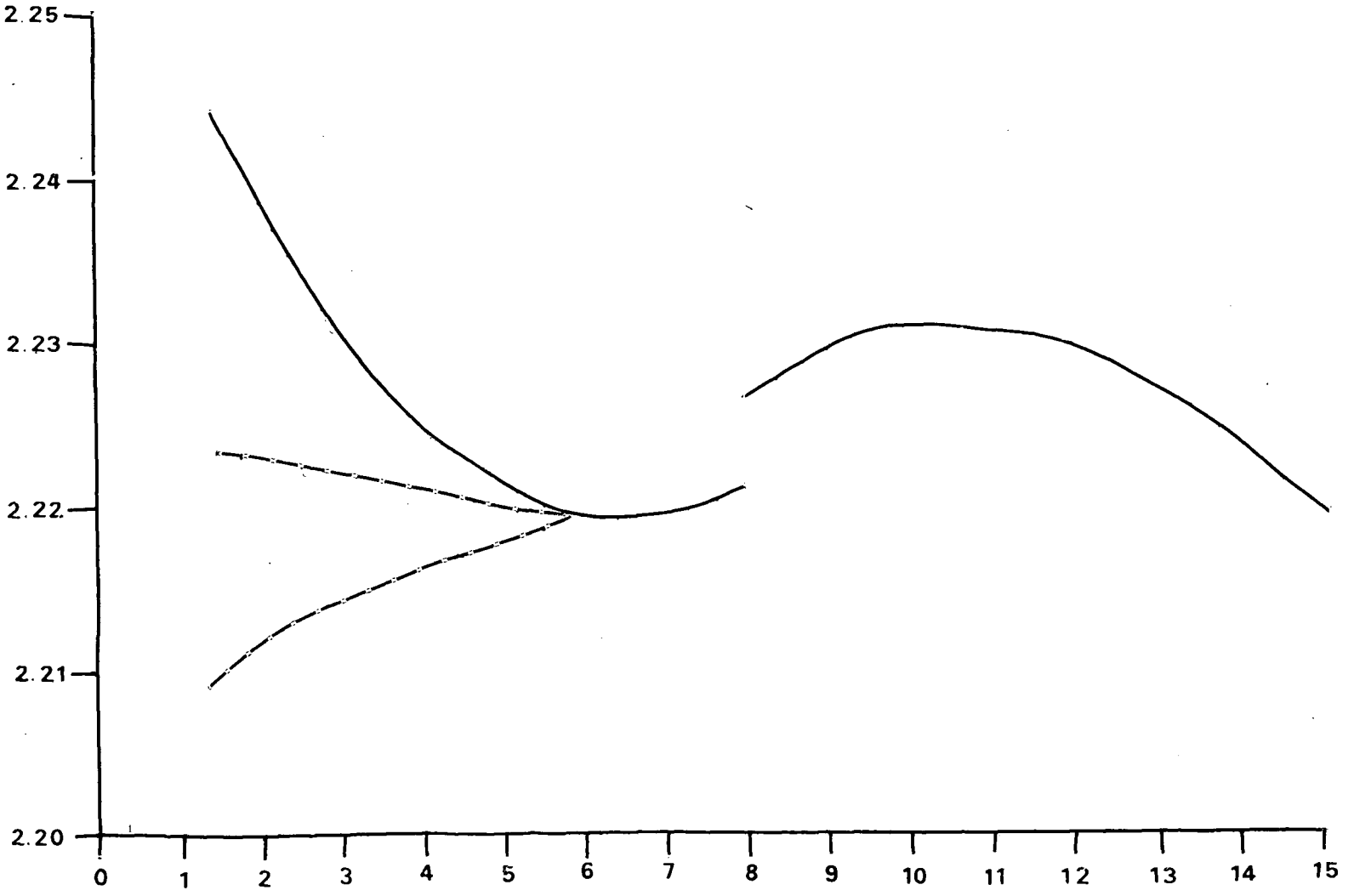

Figure 7.3. 2p Parameter versus Internuclear Distance in Bohr Radii. Upper dotted curve is $2p\sigma$. Lower dotted curve is $2p\pi$, $2p\tilde{\pi}$.

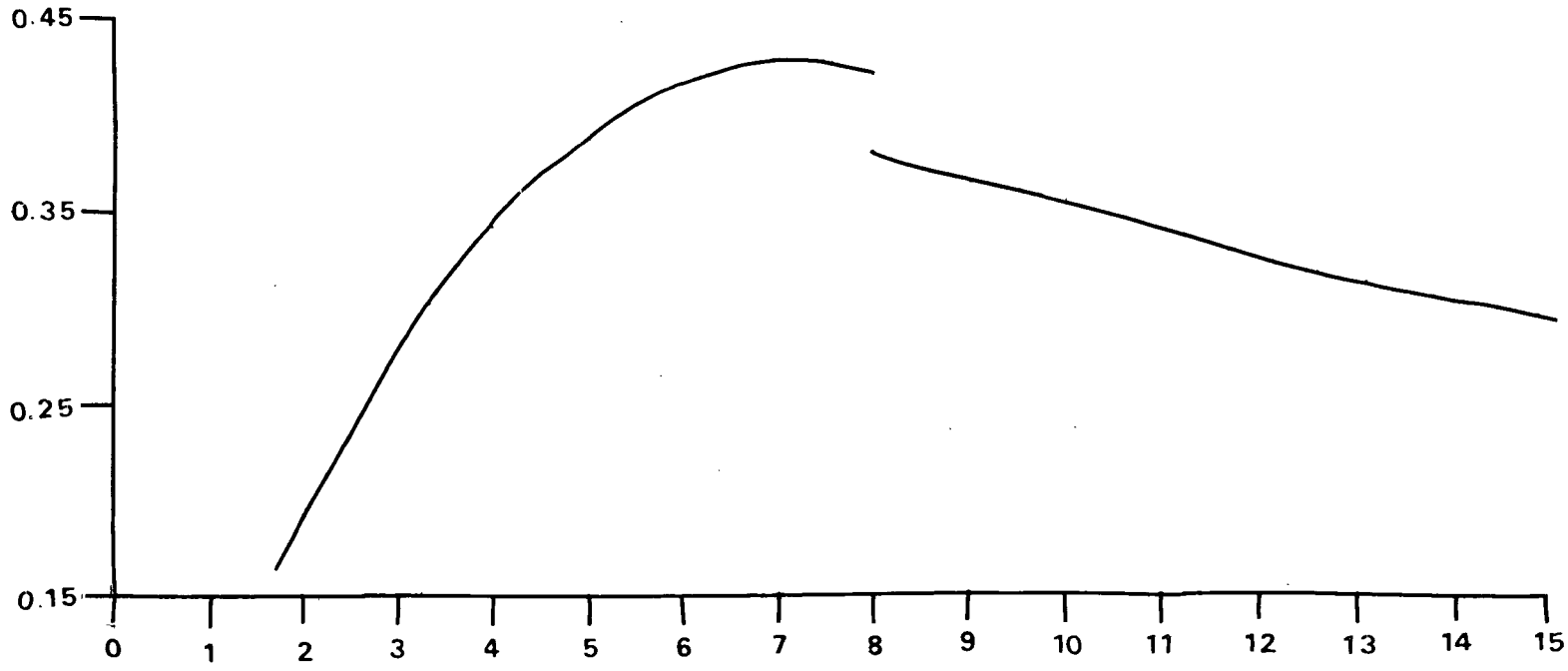

Figure 7.4. 3s Parameter versus Internuclear Distance in Bohr Radii.

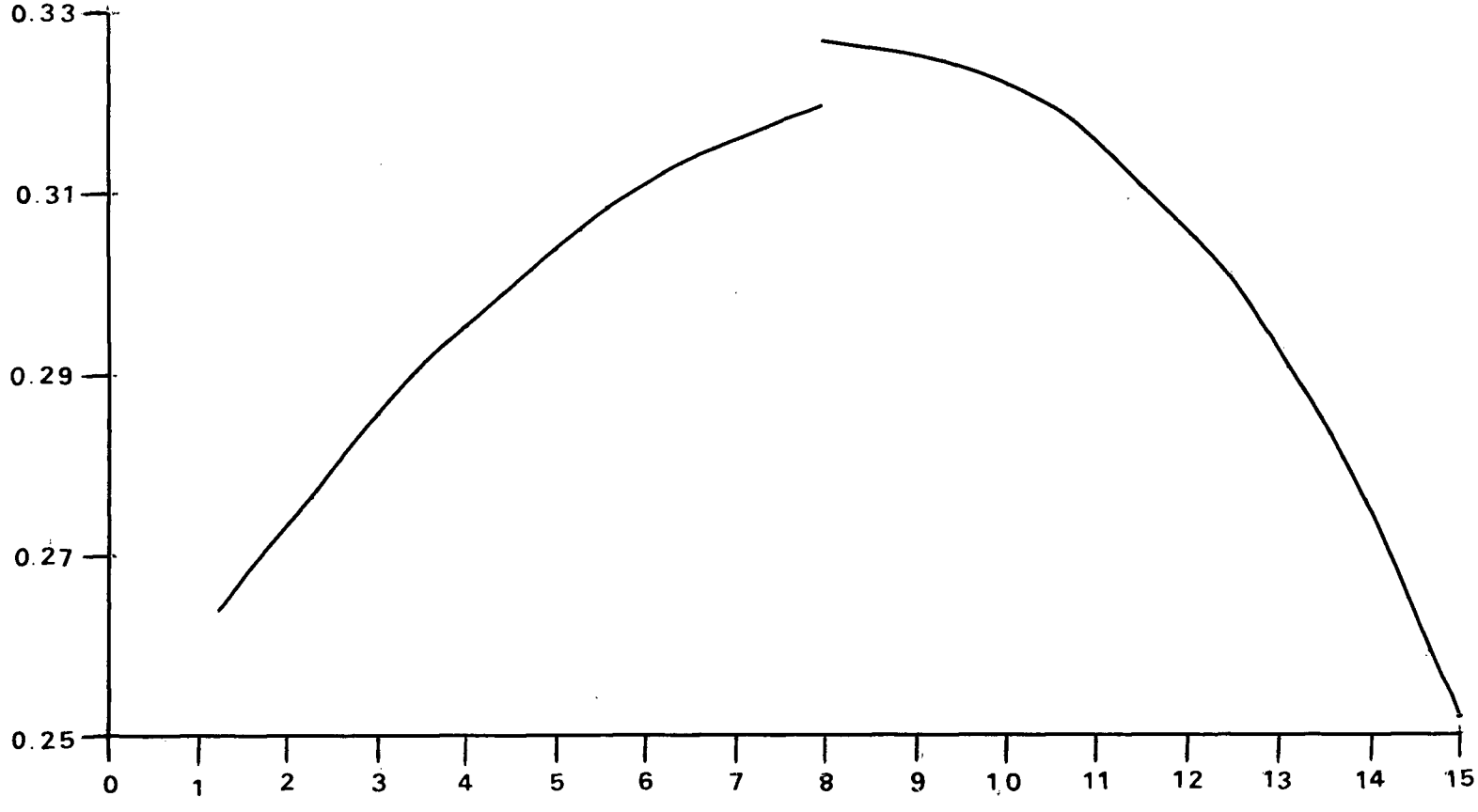

Figure 7.5. 3p Parameter versus Internuclear Distance in Bohr Radii.

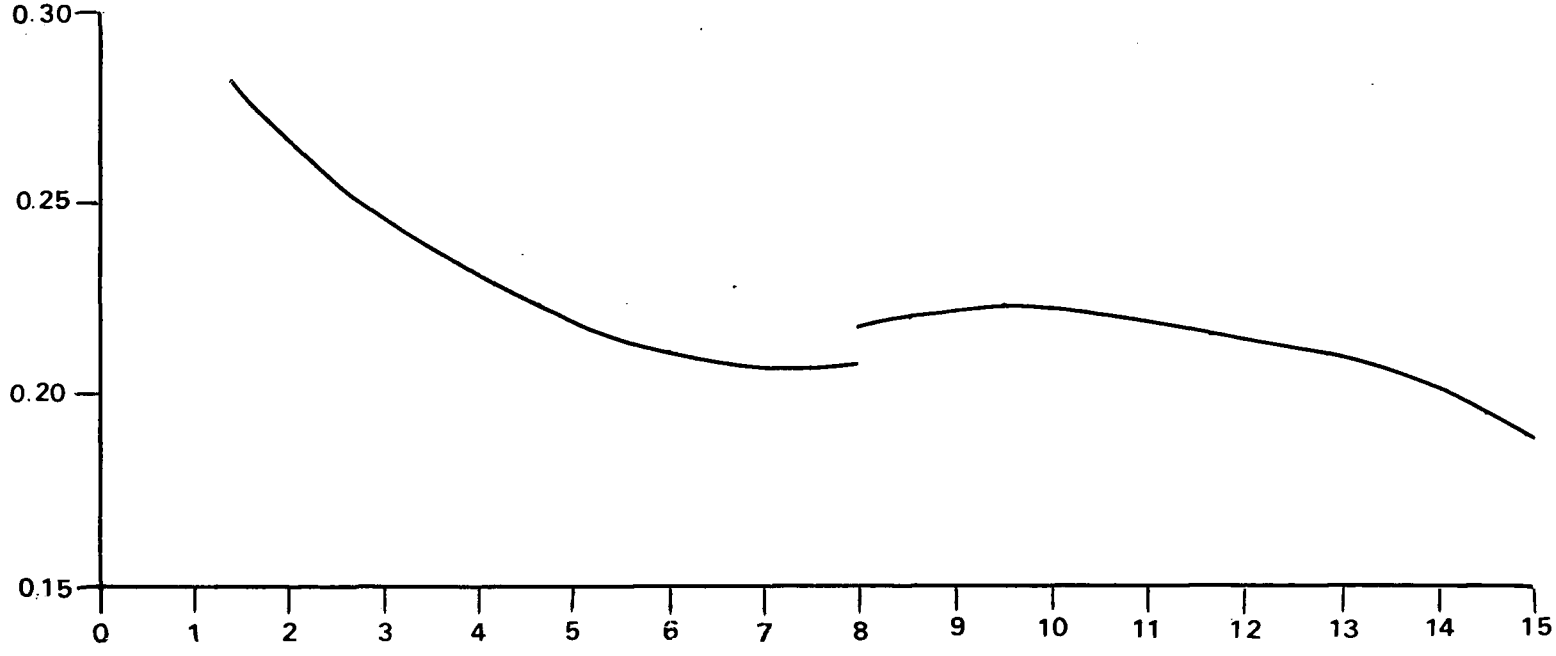

Figure 7.6. 3d Parameter versus Internuclear Distance in Bohr Radii.

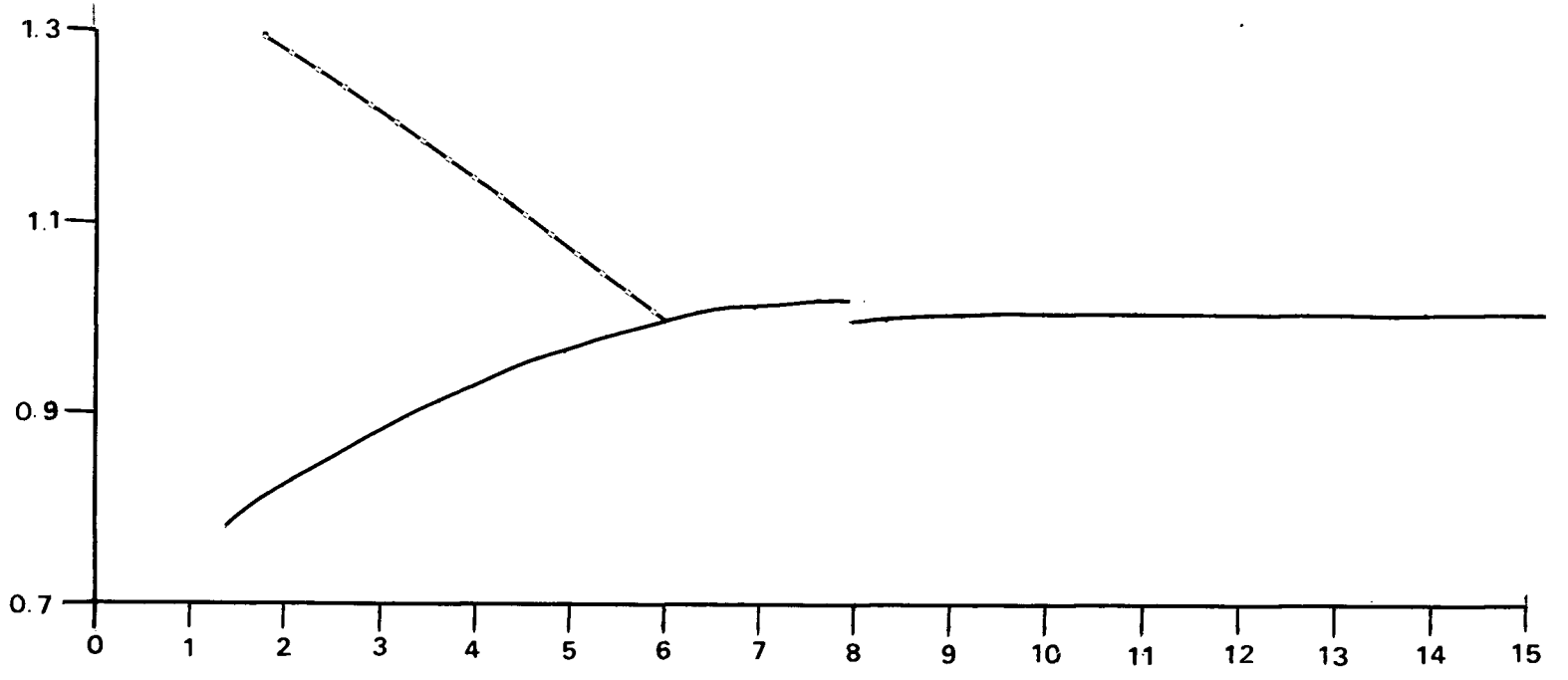

Figure 7.7 $(1s)_H$ Parameter versus Internuclear Distance in Bohr Radii. Dotted line from refined calculation of ground state.

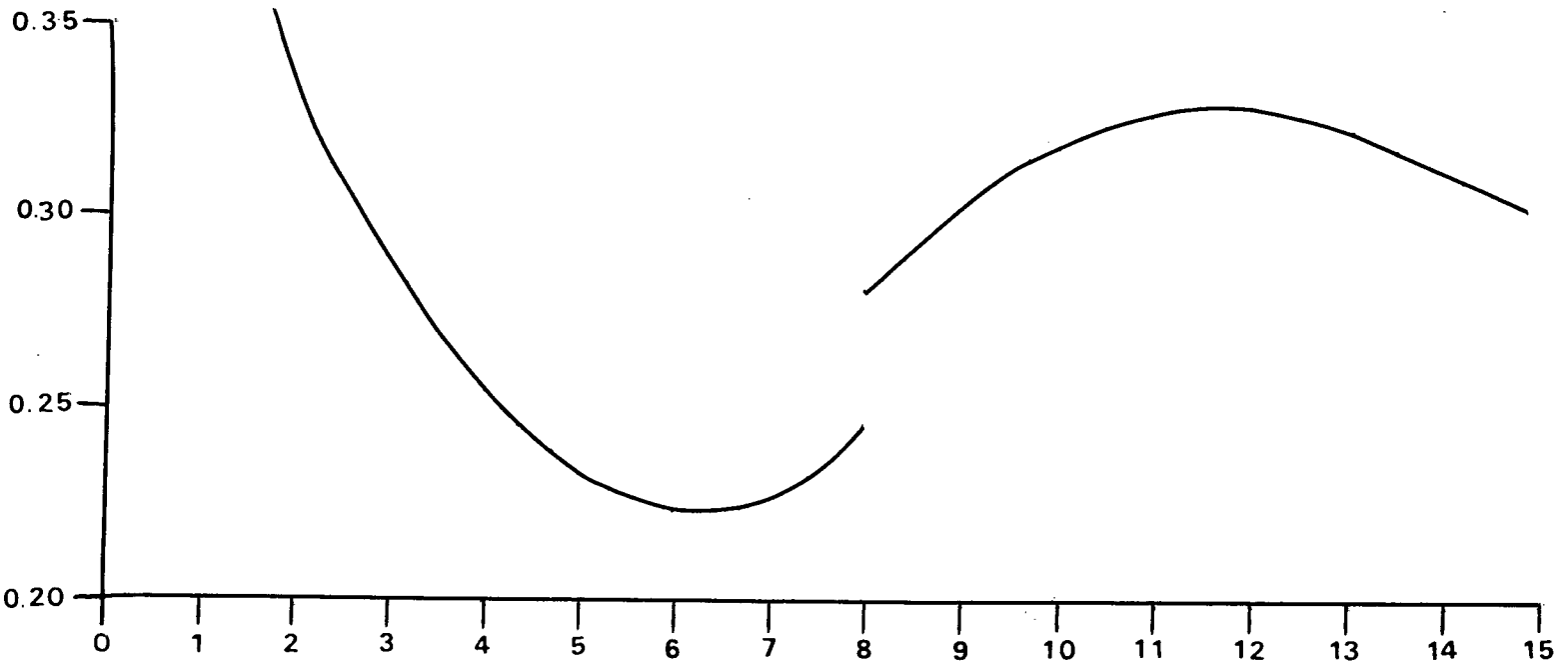

Figure 7.8. $(2s)_H$ Parameter versus Internuclear Distance in Bohr Radii.

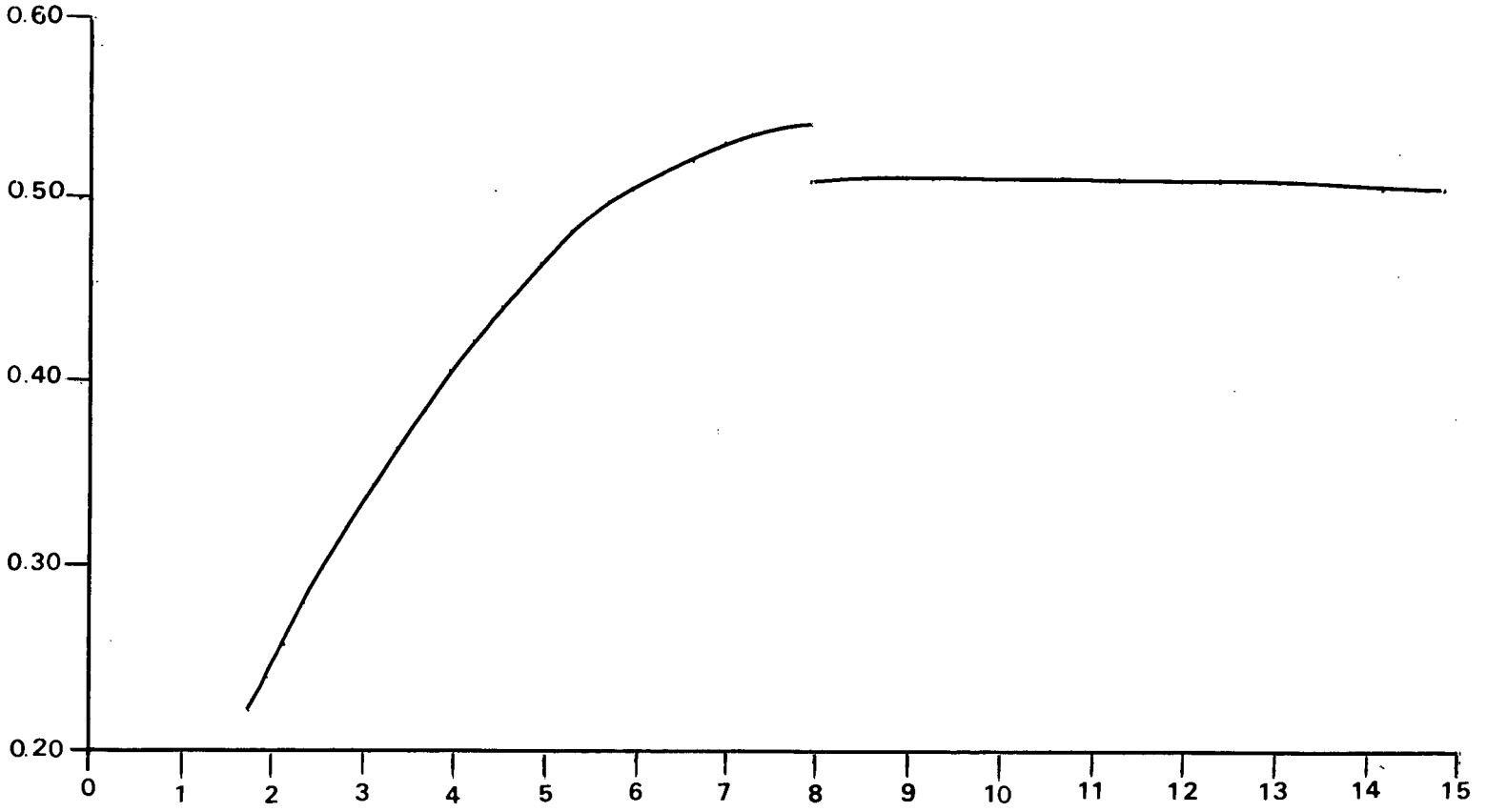

Figure 7.9. $(2p)_H$ Parameter versus Internuclear Distance in Bohr Radii.

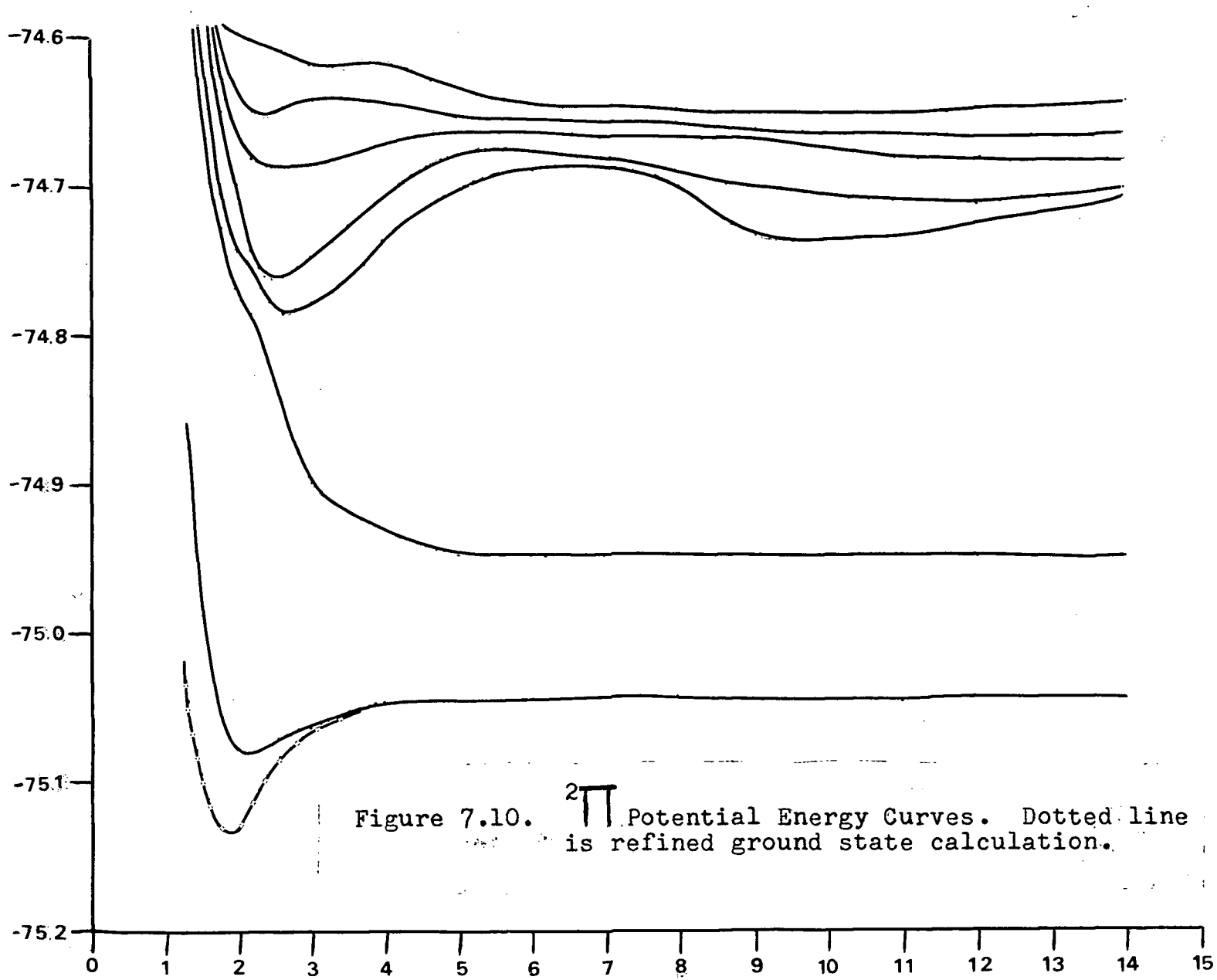

Figure 7.10. $^2\Pi$ Potential Energy Curves. Dotted line is refined ground state calculation.

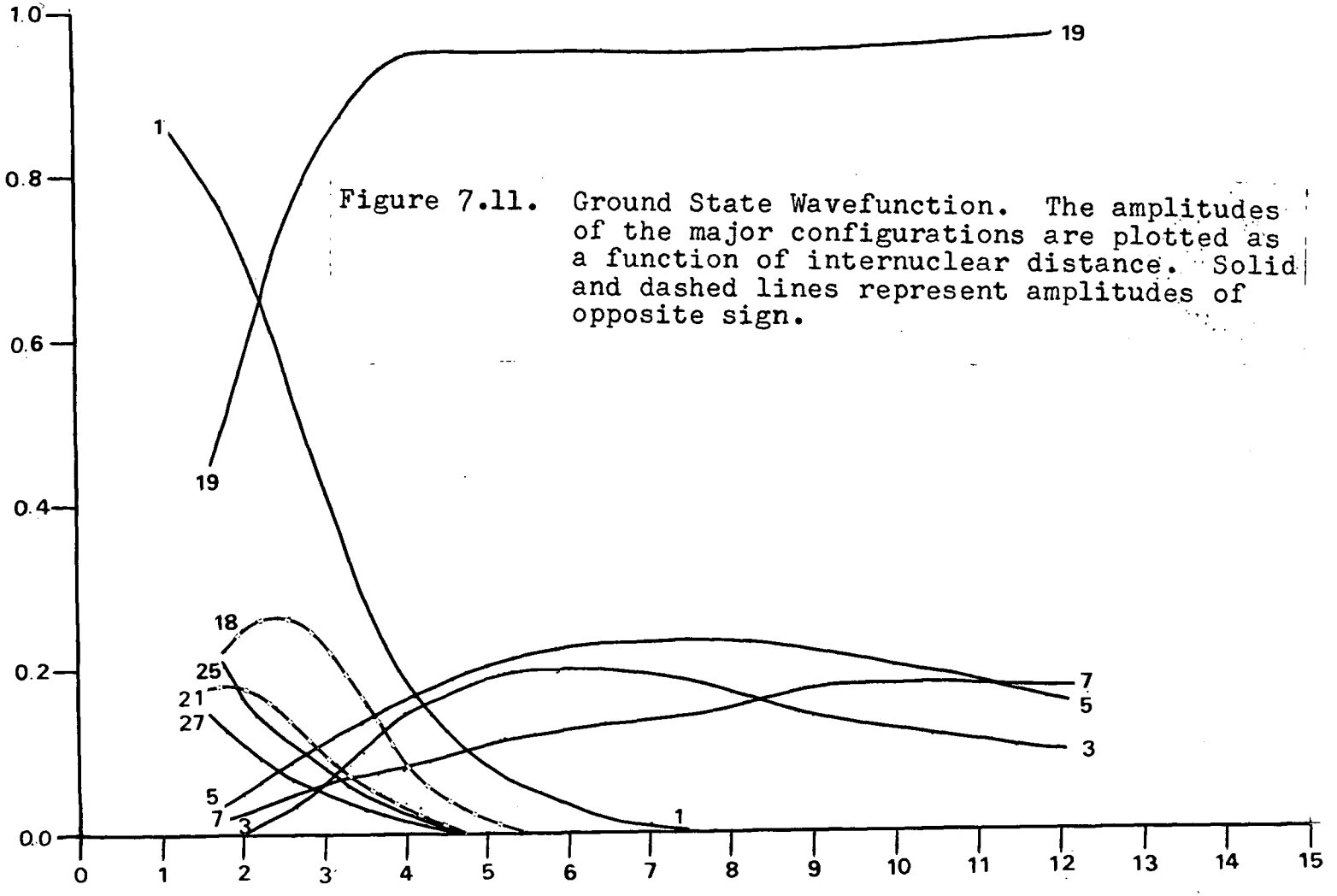

Figure 7.11. Ground State Wavefunction. The amplitudes of the major configurations are plotted as a function of internuclear distance. Solid and dashed lines represent amplitudes of opposite sign.

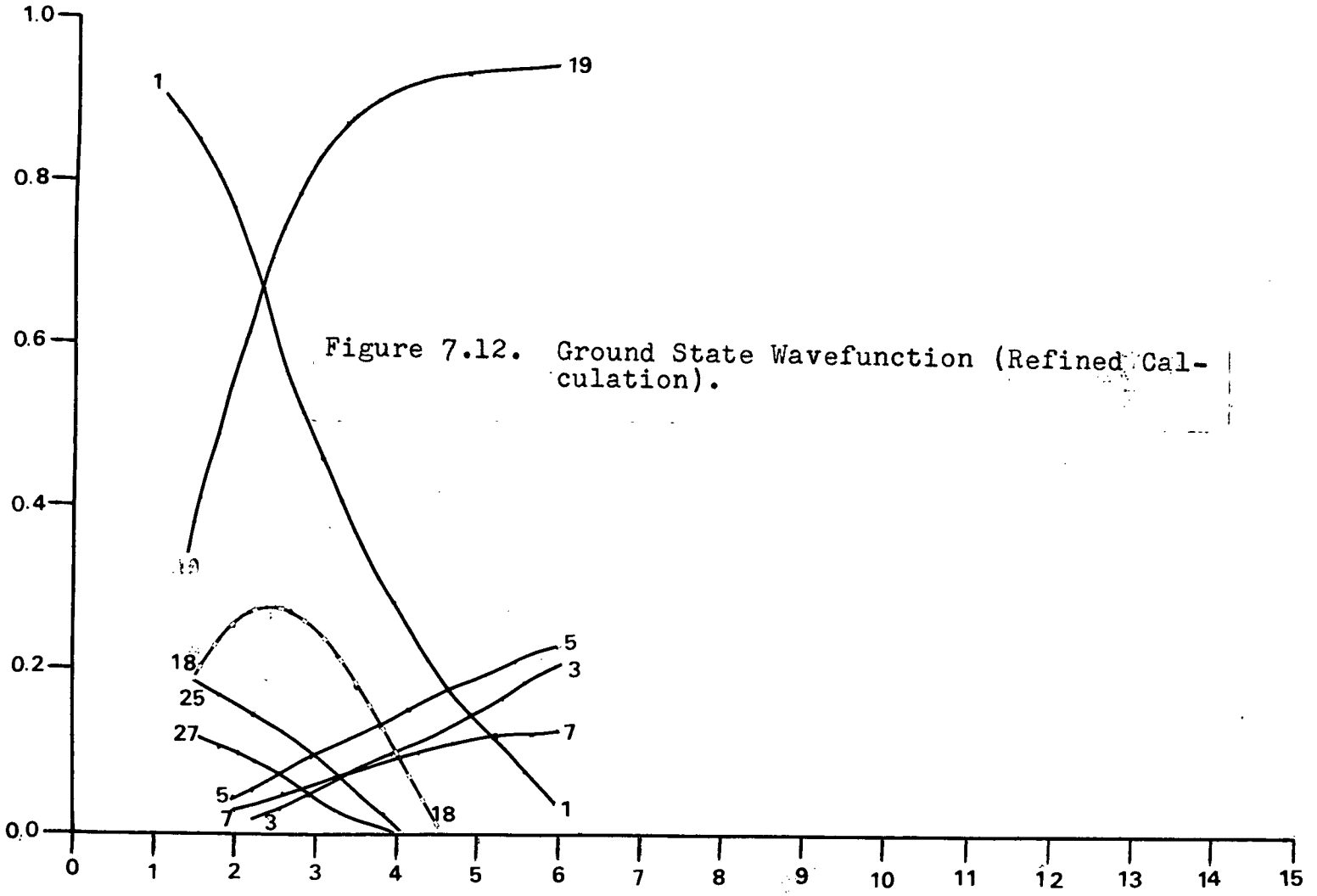

Figure 7.12. Ground State Wavefunction (Refined Calculation).

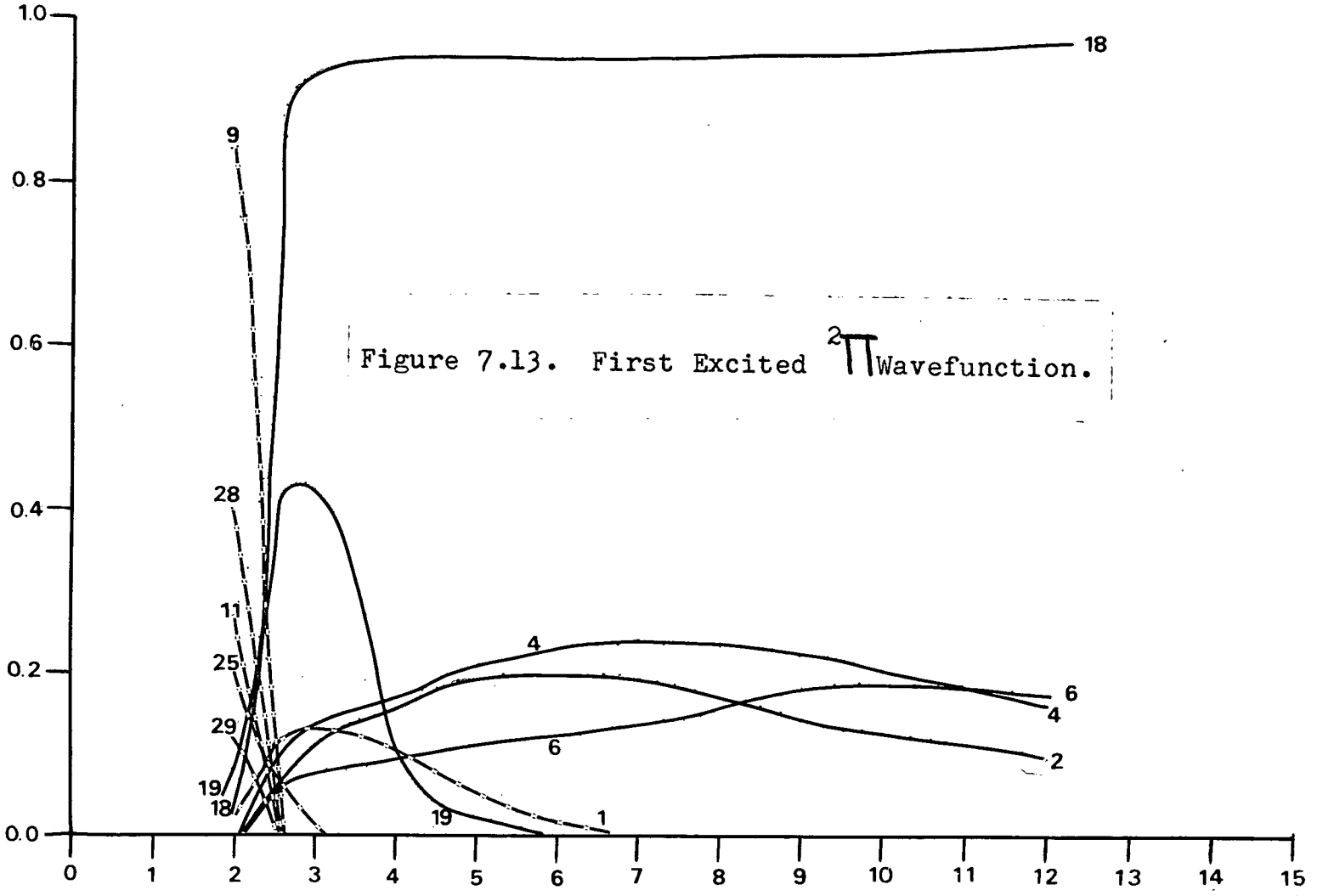

Figure 7.13. First Excited $^2\Pi$ Wavefunction.

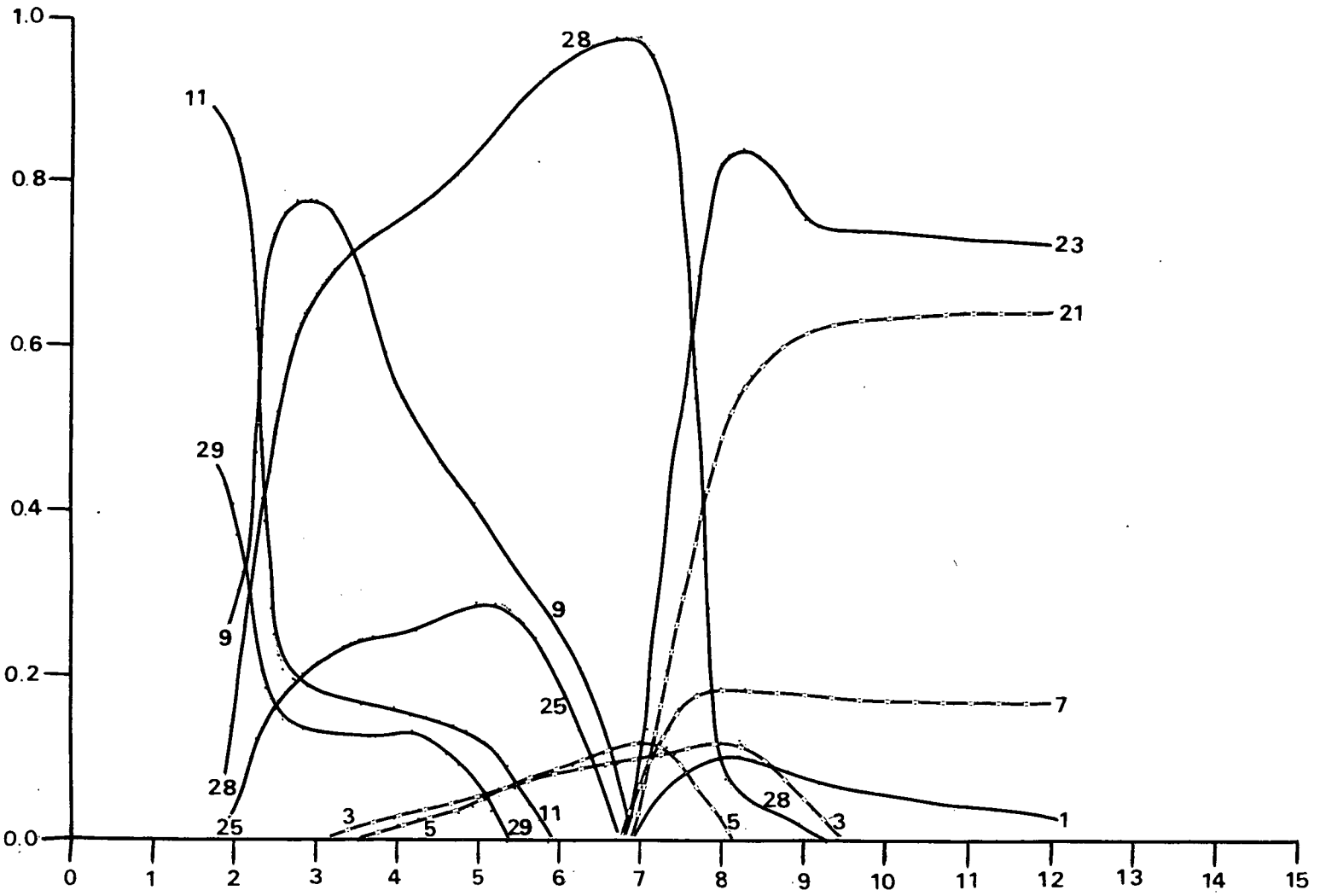

Figure 7.14. Second Excited $^2\Pi$ Wavefunction.

CHAPTER VIII
$^2\Sigma^-$ CALCULATION

1. Outline of Calculation

The second class of states for which calculations were performed is the class of $^2\Sigma^-$ states. This class was chosen because there is some indication that the lowest $^2\Sigma^-$ state is bound (Pryce, 1971).

The configurations chosen for the calculations are listed in Table 8.1. Several things from this table should be noted.

All configurations which should be present according to the guidelines laid down in Chapter IV, Section 4 are present. In addition, there is one configuration, #34, in which the 2σ orbital is singly occupied. This configuration can be obtained from configuration #9, an important constituent of the lowest $^2\Sigma^-$ state*, by moving one of the two electrons in the 2σ orbital into a 7σ orbital. It was hoped that the effectiveness of the 'frozen-core' approximation could be tested by determining the importance of this configuration to the ground state. More will be said about this in Section 2 of this chapter.

All permissible spin couplings were used in the $^2\Sigma^-$ calculations, in contrast to the $^2\Pi$ calculations.

---

* See Figure 8.11 for the wavefunction of this state.

Not all possible spin couplings are permissible, however. As noted in Chapter IV, Section 7, some of them lead to identically vanishing $^2\Sigma^-$ states. This is why, for example, spin couplings V-4 and V-5 are never used on $(1\bar{\pi})(1\pi)(3\sigma)(4\sigma)(7\sigma)$.

The average of the lowest five eigenvalues, $\bar{V}$, was minimized at R=1.8 and 6 with respect to the orbital parameters ζ_i. All $2\ell+1$ parameters which belong to the same group of atomic orbitals, as explained in the last chapter, were constrained to be equal. At R=3.5, a set of parameter values was determined by linear interpolation. Keeping the parameters for the 1s, 2s, and 2p atomic orbitals fixed at these values, $\bar{V}$ was minimized by varying the parameters for the 3s, 3p, 3d, $(1s)_H$, $(2s)_H$, and $(2p)_H$ atomic orbitals. Fixing the 1s, 2s, and 2p parameters at their interpolated values was felt to be reasonable, since the fractional changes in these parameters as R varies should be smaller than those of the other atomic orbitals. This is the case for the $^2\Pi$ calculation.

The resulting parameter values as functions of R are shown in Figures 8.1 to 8.9. The five lowest $^2\Sigma^-$ potential energy curves are shown in Figure 8.10.

More refined calculations for the lowest and second lowest $^2\Sigma^-$ states were performed. The lowest eigenvalue was minimized at R=2.1, 3.5, and 6. The second

lowest eigenvalue was minimized at R=2 and 6.* The values for those parameters which were varied are shown in Figures 8.3, 8.4, and 8.7. The two potential energy curves are shown in Figure 8.10.

2. The Lowest $^2\Sigma^-$ State

The two calculated potential energy curves for the lowest energy $^2\Sigma^-$ state are shown in Figure 8.10. The more refined calculation produces the lower curve, of course.

Both curves show the same qualitative behavior. The state is predicted to be bound, with an equilibrium separation of $R \approx 3.5$. The calculated depth of the minimum, however, is quite different in the two calculations. The cruder calculation gives about .09 Hartrees, and the more refined one .05 Hartrees.

The spectrum of OH (Pryce, 1971) seems to indicate that the state is bound by $\gtrsim$.01 Hartrees. Only a lower limit may be given with certainty because only one vibrational level has been detected, and it may not be the lowest level. If it is in fact the lowest level, then the spacing of the observed rotational levels indicates that the equilibrium separation is at R=3.1.

The present calculations can be reconciled with observation in at least two ways. In the first way, it is accepted that the observed vibrational level is the lowest

---

* See Appendix 3 for further comments on this.

one. This implies that the more refined calculation is not yet accurate enough. Since the amount of binding is lower in the more refined calculation, it is conceivable that a better calculation would predict an even lower binding energy of $\lesssim .04$ Hartrees, consistent with a figure of .01 Hartrees. It is also conceivable that this better calculation would shift the predicted equilibrium separation to < 3.5. It should be recalled that a similiar shift occured in the $^2\Pi$ ground state calculations.

In the second way, it is accepted that the calculated amount of binding and the calculated equilibrium separation are roughly correct. This implies that the observed level is a high vibrational level. An apparent equilibrium separation of 3.1 can be produced if, contrary to the present calculations, the potential energy curve rises more rapidly for $R > 3.5$ than for $R < 3.5$. It may be objected that a more usual behavior for the potential energy curves is for them to rise more rapidly for R < equilibrium separation than for R > equilibrium separation. This behavior is produced by the 8/R term in H. However, since an equilibrium separation of 3.5 is somewhat larger than the more usual value of $R \approx 2$, this objection is not a strong one.

The wavefunction for the lowest $^2\Sigma^-$ state is shown in Figure 8.11. This is the result of the first, less refined calculation. As is the case for the $^2\Pi$ ground state,

the amplitudes are practically the same in both the first and more refined calculation. That is why the amplitudes for the more refined $^2\Sigma^-$ calculation are not shown here.

For $R<2.1$, the dominant configurations are #2 and #1. The combined effect of these two is a wavefunction centred on the oxygen nucleus and consisting of a single electron in an excited orbital, plus a core of unexcited OH^+. The excited orbital is mostly $3p\sigma$ with some 3s character. The $p\sigma$ nature of the orbital can be understood as due to the lobe pulled out along the internuclear axis by the hydrogen nucleus.

At R=2.1, there is an abrupt change in the wavefunction. Configuration #9, which dissociates into oxygen and hydrogen in their ground states, is the predominant configuration for $R>2.1$. This is to be expected, since the lowest energy $^2\Sigma^-$ state at large internuclear distances is formed from oxygen in its ground (^3P) state and hydrogen in its ground (^2S) state.

What is highly interesting in the region $2.1<R<5$ is configuration #11, which dissociates into oxygen in its ground state and hydrogen with its electron in a $(2p\sigma)_H$ orbital. It is the second most important configuration in this region, and is completely unimportant elsewhere. It is precisely in this region where the state is bound. Furthermore, it is in the immediate region of the

equilibrium separation that #11 is most important. It is reasonable, then, to attribute the boundedness of the state to this configuration.

For R >6, the only configurations of note besides #9 are #1, #2, and #3, which are very similar to the three configurations in the $^2\Pi$ calculations centred on oxygen with one very diffuse orbital.

The lowest $^2\Sigma^-$ state and the ground $^2\Pi$ state are degenerate at large R. It is not surprising, then, that the calculated energies at infinite separation are the same, as can be seen by comparing Figures 7.10 and 8.10.

Configuration #34 is not a major component of the wavefunction at any value of R of interest. It could be important only at such small R that the hydrogen nucleus affects the 2σ orbital significantly. Thus the 'frozen-core' approximation is a good one except possibly at very small R.

Finally, it should be mentioned that a previous calculation (Michels and Harris, 1969) on the lowest $^2\Sigma^-$ state predicted that the state is unbound. That calculation, in the light of what has been said in this section, is most probably incorrect.

3. The Second Lowest $^2\Sigma^-$ State

The two calculated potential energy curves for the second lowest $^2\Sigma^-$ state are shown in Figure 8.10. Both calculations predict that the state is bound at $R \approx 2.1$, and that the potential energy curve has a maximum at $R=4$.

One vibrational level of a $^2\Sigma^-$ state with an equilibrium separation at $R \approx 2$ has recently been observed (Douglas, 1971). The energy difference between this level and the observed level in the lowest $^2\Sigma^-$ state (Pryce, 1971) is very nearly .20 Hartrees, the energy difference as calculated from Figure 8.10. It seems quite certain, then, that the state observed by Douglas is the first excited $^2\Sigma^-$ state.

Another excited $^2\Sigma^-$ state has been observed (Pryce, 1971). It has an equilibrium separation of $R=3.7$, and the minimum in its potential energy curve lies above the calculated minimum of the first excited $^2\Sigma^-$ state but below the calculated maximum. The present calculations are therefore completely unable to account for the existance of this other excited state. A possible explanation, however, will be offered later in this section.

The wavefunction for the first excited $^2\Sigma^-$ state as obtained from the first calculation is shown in Figure 8.12. As noted previously, the amplitudes change little in a more refined calculation, and therefore the more refined

wavefunction is not shown.

For $R<2.1$, the wavefunction is effectively that of an electron in an excited orbital, plus an unexcited OH^+ core. The orbital is mostly 3s, with some $3p\sigma$ character*. It had been guessed (Douglas, 1971) that at the equilibrium separation, this orbital is probably 3s, but that it could possibly be $3p\sigma$. Figure 8.12 shows that the orbital is in fact an almost equal mixture of 3s and $3p\sigma$ at that distance.

For $2.1<R<3.6$, this orbital is almost purely $3p\sigma$. As $R\rightarrow 3.6$, an electron which at smaller separations occupies a $2p\sigma$ atomic orbital on oxygen begins to detach itself and occupies a $(1s)_H$ atomic orbital. This is evidenced by the increasing importance of configuration #15.

At R=3.7, there is a change in the nature of the wavefunction. Configuration #12, which dissociates into oxygen in an excited ($^3S^o$) state and hydrogen in its ground (^2S) state, becomes predominant. It is near this point that the potential energy curve reaches its maximum. As $R\rightarrow\infty$, the wavefunction becomes pure #12, and the potential energy curve decreases monotonically.

The existence of the other excited $^2\Sigma^-$ state (Pryce, 1971) mentioned previously can be explained if the maximum in the potential energy curve were between R=2.1 and R=3.7, and if there were a minimum near R=3.7; that is,

---

* Compare this with the description in the previous section of the lowest $^2\Sigma^-$ wavefunction for $R<2.1$.

if the two observed excited $^2\Sigma^-$ states were the same state, but corresponded to two minima in the potential energy curve.

It should be recalled that in the lowest $^2\Sigma^-$ state calculation there was a configuration, #11, which if it had been omitted from the calculation would probably have caused the state to appear to be unbound. Furthermore, the minimum in the lowest $^2\Sigma^-$ curve due to #11 is at R=3.5, very near the proposed minimum at R=3.7 in the excited $^2\Sigma^-$ state. This suggests that a configuration similar to #11 has been omitted from the present calculations, which, if it were included, would produce a minimum at the desired place in the first excited $^2\Sigma^-$ curve.

Configuration #11 can be constructed by replacing the 7σ molecular orbital in configuration #9, which is the dominant configuration for the lowest $^2\Sigma^-$ state in the region of its equilibrium separation, by a 9σ molecular orbital. A similar procedure for the first excited $^2\Sigma^-$ state near R=3.7 produces $(1\sigma)^2(2\sigma)^2(1\tilde{\pi})(1\pi)(3\sigma)(5\sigma)(9\sigma)$, with appropriate spin coupling. A calculation should be performed using this configuration.

The calculated energy difference at infinite internuclear distance between the lowest and the second lowest $^2\Sigma^-$ state is $\approx$.17 Hartrees. The actual value, which is the energy difference between the lowest $^3S^o$ and ^3P states of oxygen, or equivalently, the difference in ionization

potentials of a 2p and a 3s electron in oxygen, is closer to .42 Hartrees (Edlén, 1943). The agreement is poor.

A detailed analysis of the computer printout, which is not reproduced here, has shown that the calculated 2p ionization potential is low, and the 3s is high. These two errors add to produce the large error.

It seems that the errors arise because the program has been designed to describe molecules, but not separated atoms, well. Even a self-consistent calculation, however, (Hartree et al, 1940) fails to get a good value for the ionization potential of a 2p electron in oxygen.

4. The Third Lowest $^2\Sigma^-$ State

The wavefunction for this state is shown in Figure 8.13. It appears to be similar to the second lowest $^2\Sigma^-$ wavefunction.

At $R < 2.1$, the wavefunction is that of an electron in a $3d\sigma$ atomic orbital on oxygen, plus an unexcited OH^+ core centred on oxygen. At the equilibrium separation $R=2.2$, this orbital is a roughly equal mixture of $3d\sigma$ and 3s, with some $3p\sigma$ character. Between $2.2 < R < 3.7$, the orbital is 3s. At $R=3.7$, the molecule begins to dissociate into hydrogen in its ground state and oxygen in an excited ^3P state.

Configuration Number	Spatial Part	Spin Coupling
1	$(1\sigma)^2(2\sigma)^2(1\bar{\pi})(3\sigma)^2(1\pi)(4\sigma)$	III-2
2	$(1\sigma)^2(2\sigma)^2(1\bar{\pi})(3\sigma)^2(1\pi)(5\sigma)$	III-2
3	$(1\sigma)^2(2\sigma)^2(1\bar{\pi})(3\sigma)^2(1\pi)(6\sigma)$	III-2
4,5	$(1\sigma)^2(2\sigma)^2(1\bar{\pi})^2(3\sigma)(1\pi)(2\pi)$	III-1,2
6,7	$(1\sigma)^2(2\sigma)^2(1\bar{\pi})^2(3\sigma)(1\pi)(3\pi)$	III-1,2
8	$(1\sigma)^2(2\sigma)^2(1\bar{\pi})^2(3\sigma)^2(1\delta)$	I-1
9	$(1\sigma)^2(2\sigma)^2(1\bar{\pi})(3\sigma)^2(1\pi)(7\sigma)$	III-2
10	$(1\sigma)^2(2\sigma)^2(1\bar{\pi})(3\sigma)^2(1\pi)(8\sigma)$	III-2
11	$(1\sigma)^2(2\sigma)^2(1\bar{\pi})(3\sigma)^2(1\pi)(9\sigma)$	III-2
12,13,14	$(1\sigma)^2(2\sigma)^2(1\bar{\pi})(1\pi)(3\sigma)(4\sigma)(7\sigma)$	V-1,2,3
15,16,17	$(1\sigma)^2(2\sigma)^2(1\bar{\pi})(1\pi)(3\sigma)(5\sigma)(7\sigma)$	V-1,2,3
18,19,20	$(1\sigma)^2(2\sigma)^2(1\bar{\pi})(1\pi)(3\sigma)(6\sigma)(7\sigma)$	V-1,2,3
21,22	$(1\sigma)^2(2\sigma)^2(1\bar{\pi})(3\sigma)^2(2\pi)(7\sigma)$	III-1,2
23,24	$(1\sigma)^2(2\sigma)^2(1\bar{\pi})(3\sigma)^2(3\pi)(7\sigma)$	III-1,2
25,26	$(1\sigma)^2(2\sigma)^2(1\bar{\pi})^2(1\pi)(2\pi)(7\sigma)$	III-1,2
27,28	$(1\sigma)^2(2\sigma)^2(1\bar{\pi})^2(1\pi)(3\pi)(7\sigma)$	III-1,2
29,30	$(1\sigma)^2(2\sigma)^2(1\bar{\pi})^2(3\sigma)(1\delta)(7\sigma)$	III-1,2
31,32	$(1\sigma)^2(2\sigma)^2(1\bar{\pi})^2(3\sigma)(1\pi)(4\pi)$	III-1,2
33	$(1\sigma)^2(2\sigma)^2(1\bar{\pi})(1\pi)(3\sigma)(7\sigma)^2$	III-2
34	$(1\sigma)^2(1\bar{\pi})(3\sigma)^2(1\pi)(7\sigma)^2(2\sigma)$	III-2

Table 8.1. Configurations for $^2\Sigma^-$ Calculation

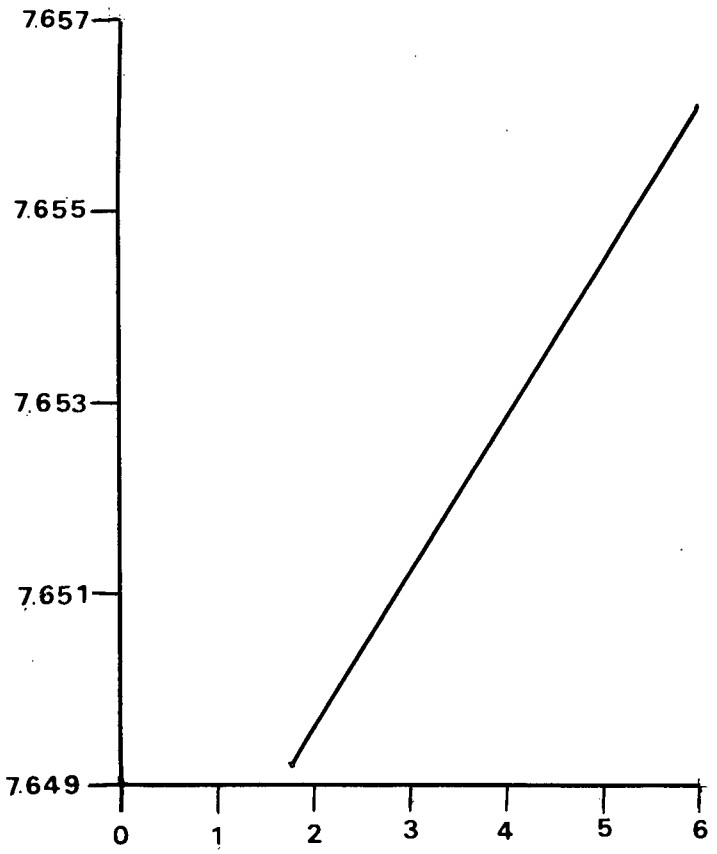

Figure 8.1. ls Parameter for $^2\Sigma^-$ States.

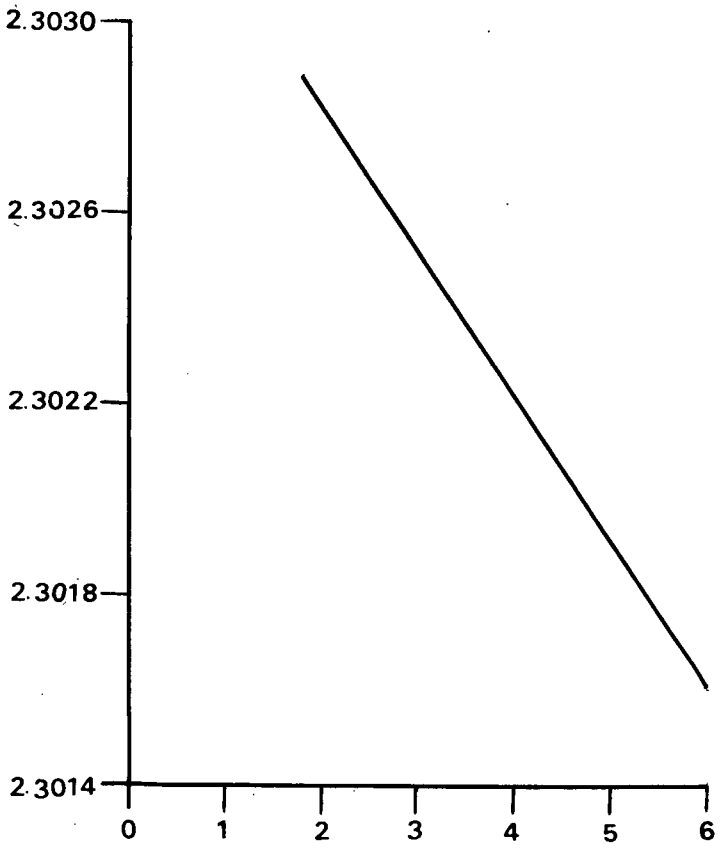

Figure 8.2. 2s Parameter.

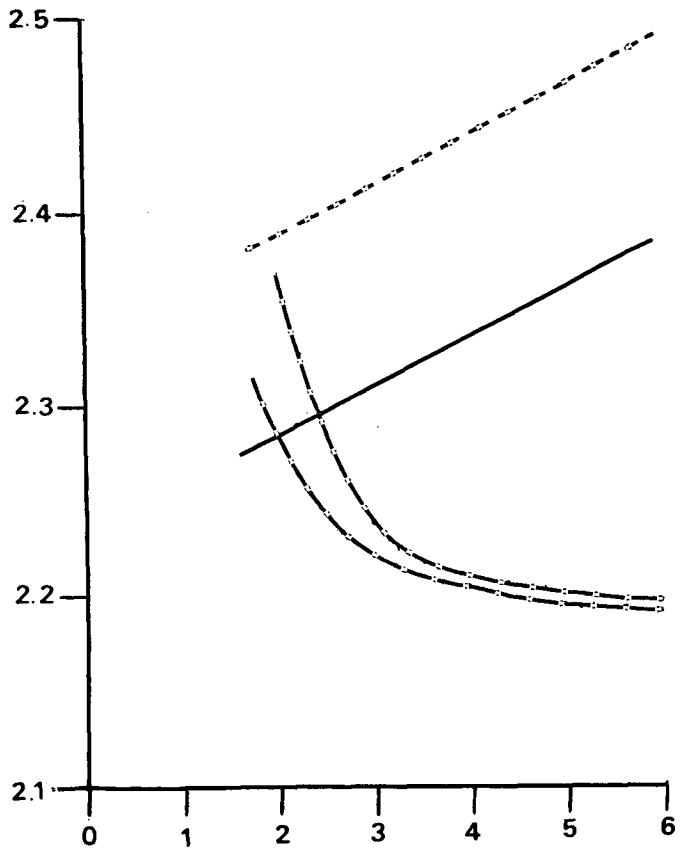

Figure 8.3. 2p Parameters for $^2\Sigma^-$ States. Lowest dotted curve is for $2p\pi$, $2p\tilde{\pi}$ parameter in lowest state. Second lowest dotted curve is for $2p\sigma$ parameter in lowest state. Upper dotted curve is for second lowest state. Solid line is for lowest five states.

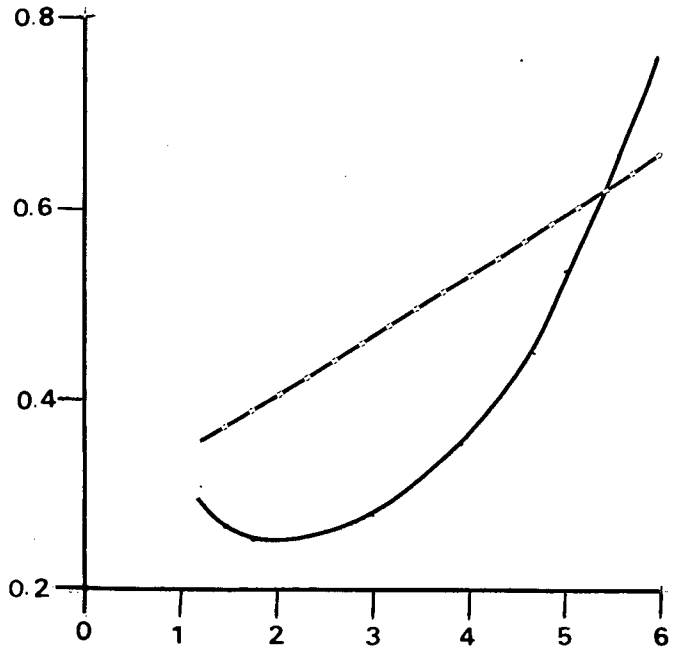

Figure 8.4. 3s Parameter. Dotted line is only for second lowest $^2\Sigma^-$ state.

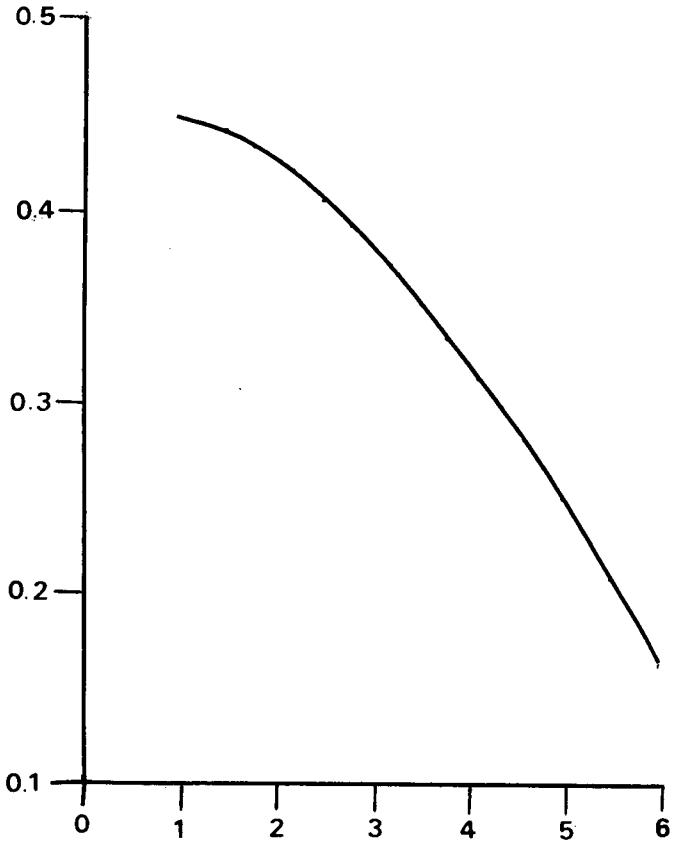

Figure 8.5. 3p Parameter.

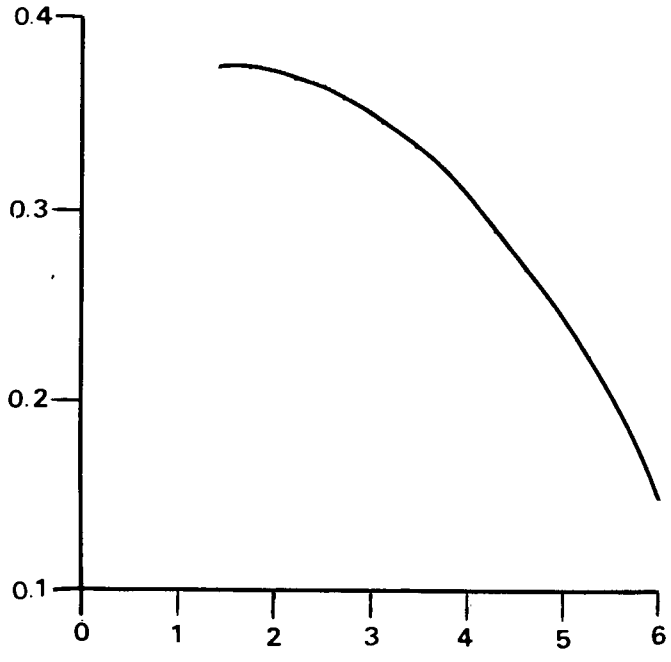

Figure 8.6. 3d Parameter

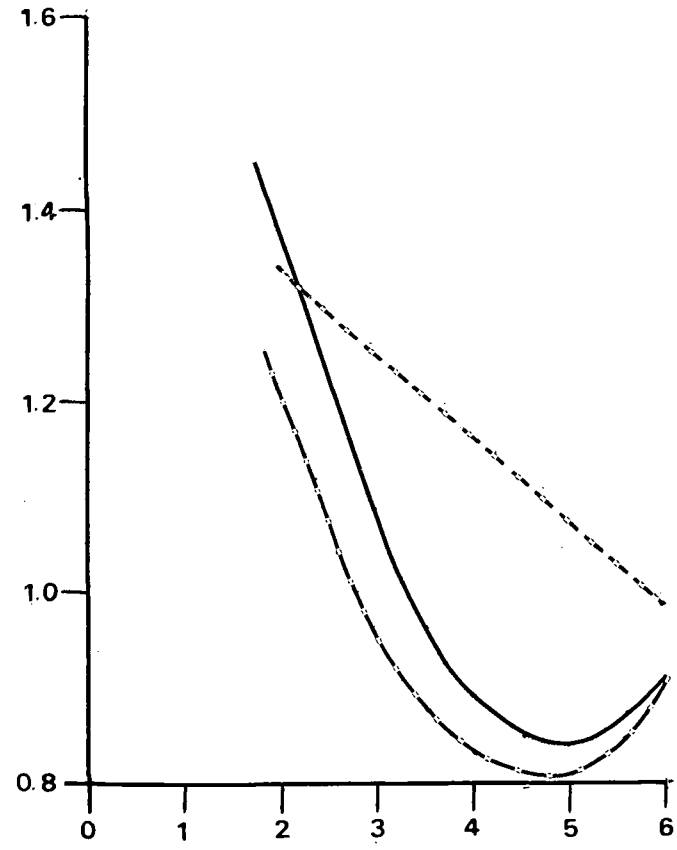

Figure 8.7. $(1s)_H$ Parameter. Lower dotted line is for lowest $^2\Sigma^-$ state. Upper dotted line is for second lowest $^2\Sigma^-$ state.

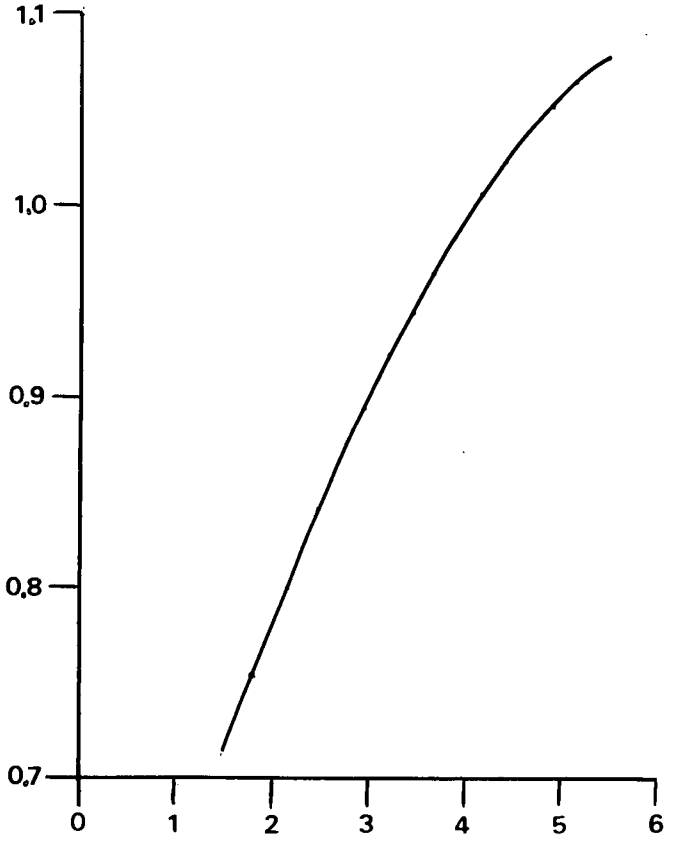

Figure 8.8. $(2s)_H$ Parameter.

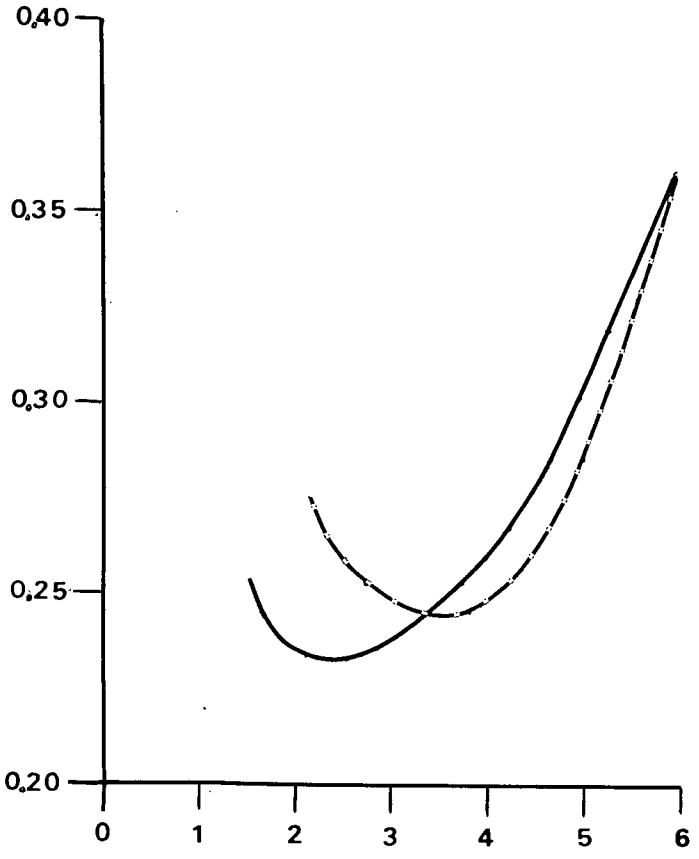

Figure 8.9. $(2p)_{^2\Sigma^-_H}$ Parameter. Dotted line is for lowest state.

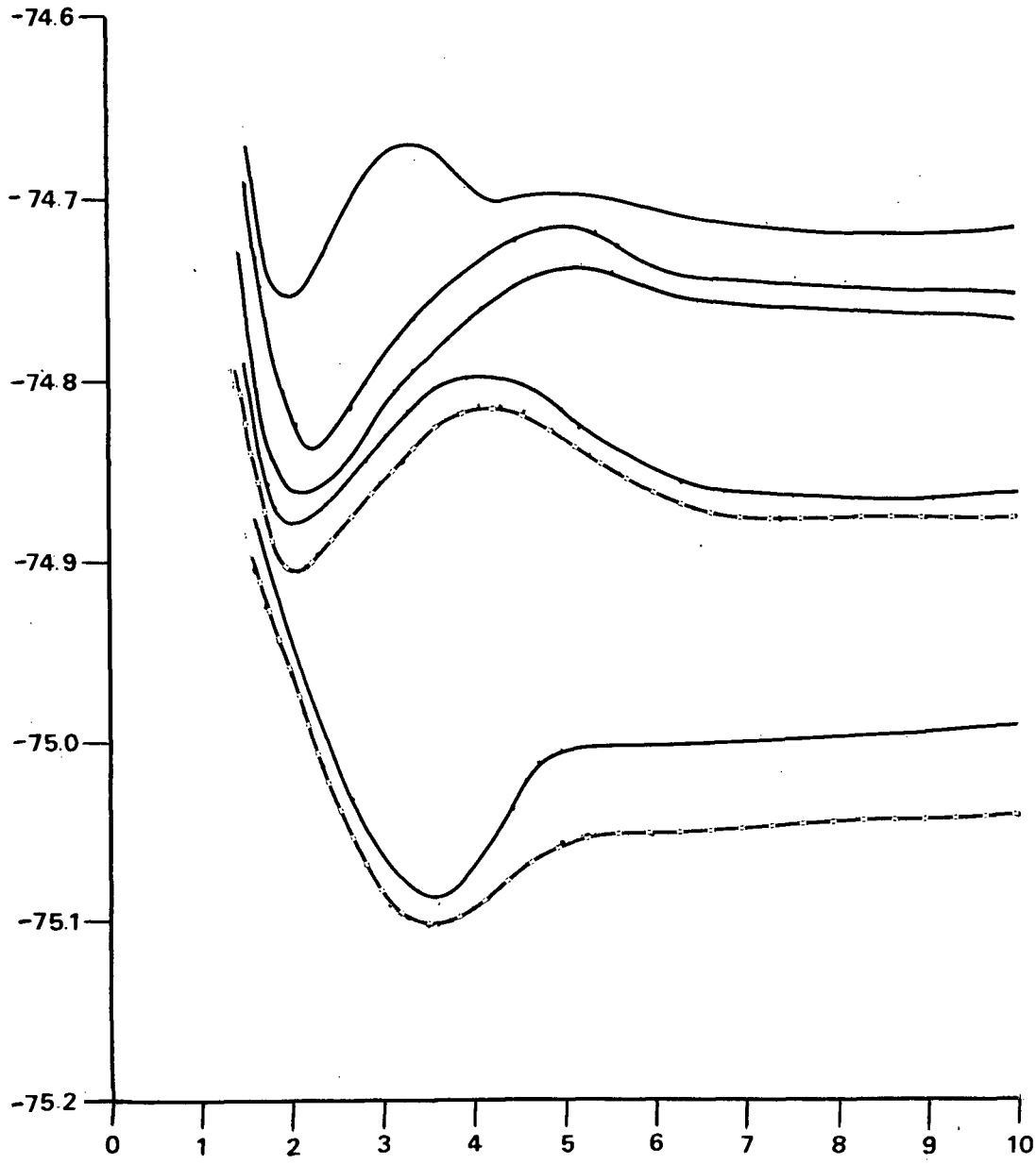

Figure 8.10. $^2\Sigma^-$ Potential Energy Curves. Dotted curves are from refined calculations on lowest and second lowest states.

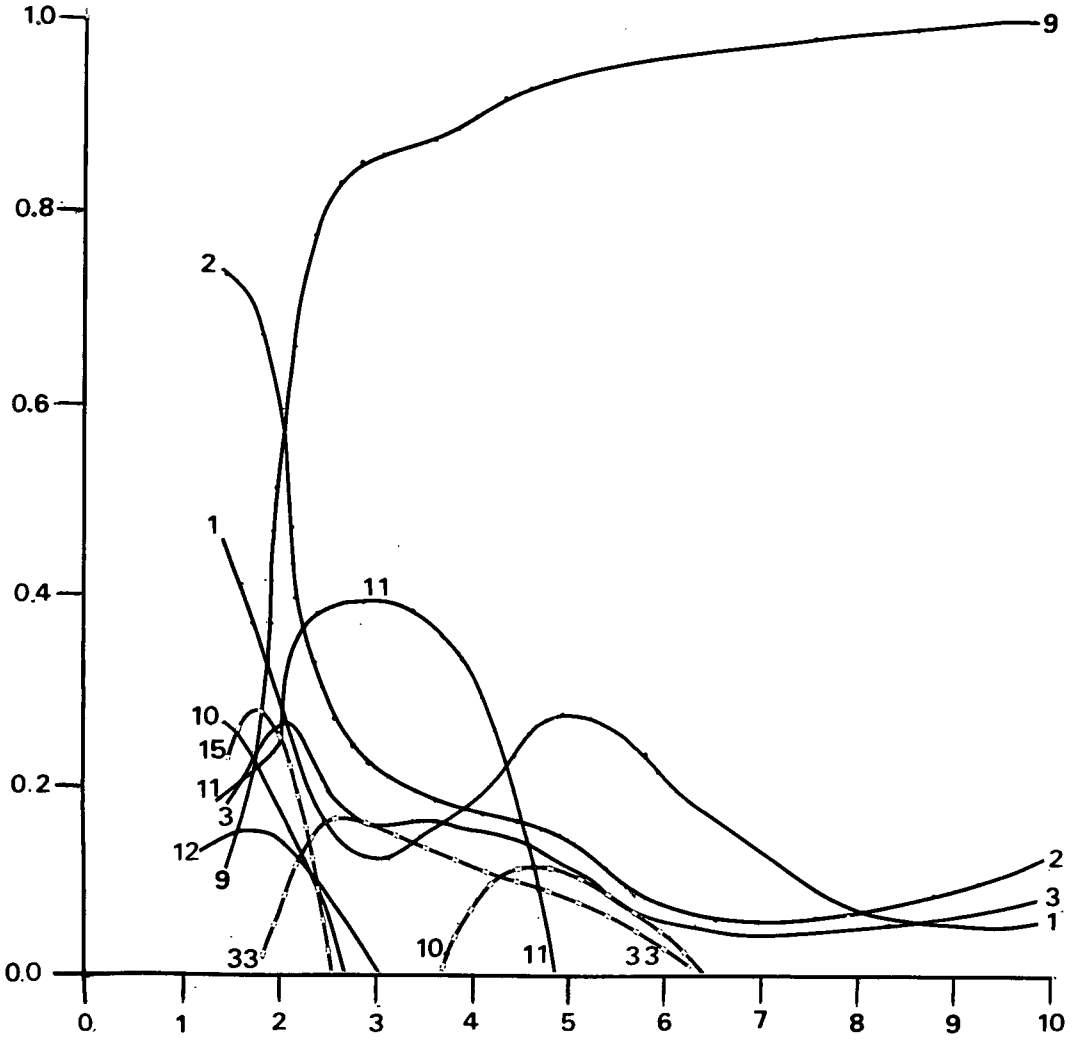

Figure 8.11. Lowest $^2\Sigma^-$ Wavefunction.

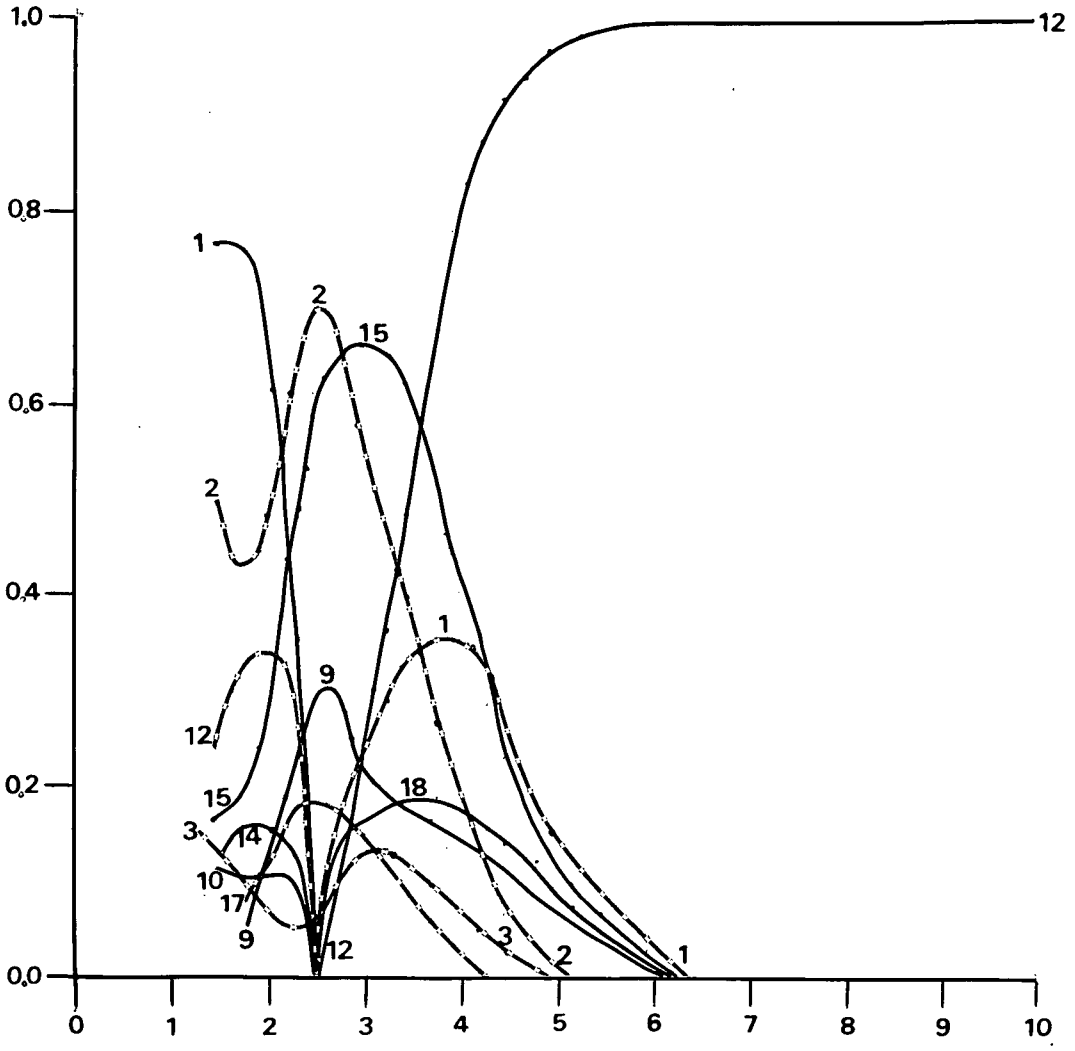

Figure 8.12. Second Lowest $^2\Sigma^-$ Wavefunction.

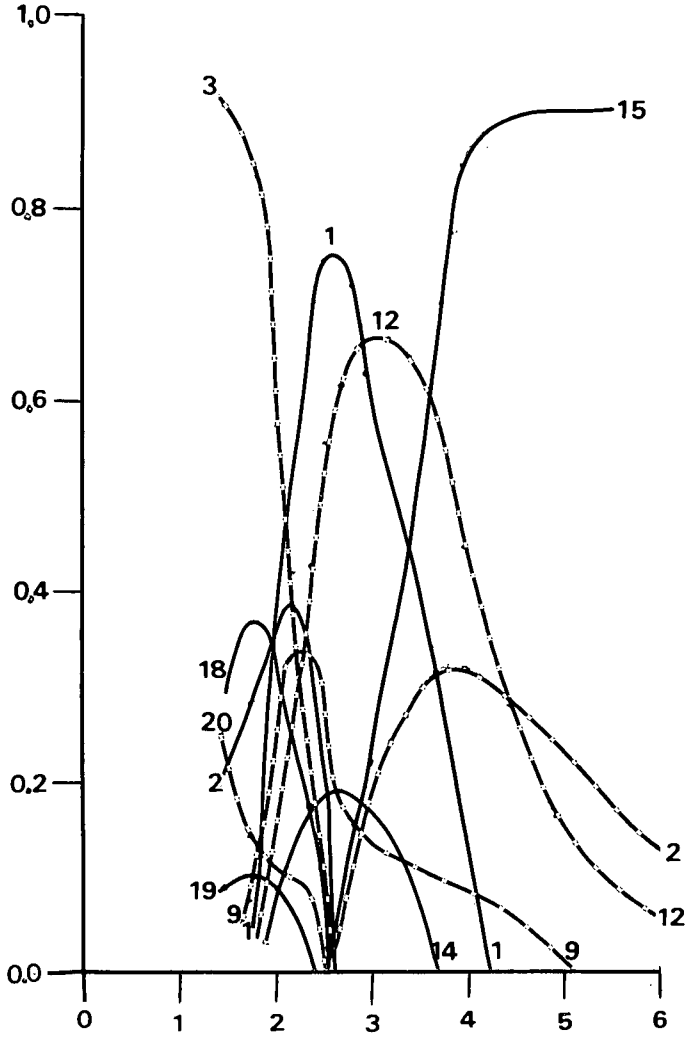

Figure 8.13. Third Lowest $^2\Sigma^-$ Wavefunction.

CHAPTER IX

CONCLUDING REMARKS

The computer programs developed here have been useful in the interpretation of the spectrum of OH, even though they have not yet been used as wisely as they could have been. In the future, calculations of the $^4\Sigma^-$, $^4\Pi$, and $^2\Delta$ states are planned. The $^2\Pi$ states will also be recalculated, and possibly the second lowest $^2\Sigma^-$ calculation will be redone.

BIBLIOGRAPHY

Born, M., and Oppenheimer, J.R., Ann. der Phys. 84, 457 (1927).

Carlone, C., Spectrum of the Hydroxyl Radical, Ph.D. Thesis, University of British Columbia, 1969.

Condon, E.U., and Shortley, G.H., The Theory of Atomic Spectra, Cambridge Univ. Press, 1951.

Douglas, A.E., "Absorption of OH in the 1200 Å Region", to be published (1971).

Edlen, B., Kungl. Svenska Vetenskapsakad. Handl. 3 , 20, No. 10 (1943).

Harris, F.E., J. Chem. Phys. 51, 4770 (1969).

Hartree, D.R., Hartree, W., and Swirles, B., Phil. Trans. Roy. Soc. A 238, 229 (1940).

Herzberg, G., The Spectra and Structures of Simple Free Radicals, Cornell Univ. Press, 1971.

Joy, H.W., and Parr, R.G., J. Chem. Phys. 28, 444 (1958).

Michels, H.H., and Harris, F.E., Chem. Phys. Lett. 3, 441 (1969).

Powell, M.J.D., Comp. Jour. 7, 1955 (1964).

Pryce, M.H.L., "Steps in Analysis of OH Spectrum, 53,000-58,000 cm^{-1}", unpublished notes (1971).

Slater, J.C., Quantum Theory of Atomic Structure, V.1, McGraw-Hill, 1960.

Switendick, A.C., and Corbato, F.J., in Methods of Computational Physics, II, Academic Press, 1963.

Terzian, Y., and Scharlemann, E., Earth and Terr. Sci. 1, 103 (1970).

APPENDIX 1

MATRIX ELEMENTS OF H BETWEEN SLATER DETERMINANTS

The diagonal matrix elements are

$$\int S_k^* \, h_0 \, S_k dV = h_0 \quad , \tag{A1.1}$$

$$\int S_k^* \left(\sum_i h_1^{(i)}\right) S_k dV = \sum_i \langle \chi_i' | h_1 | \chi_i' \rangle \quad , \tag{A1.2}$$

and

$$\int S_k^* \left(\tfrac{1}{2} \sum_{i \neq j} h_2^{(i,j)}\right) S_k dV = \tfrac{1}{2} \sum_{i \neq j} \left[\langle \chi_i', \chi_j' | h_2 | \chi_i', \chi_j' \rangle - \langle \chi_i', \chi_j' | h_2 | \chi_j', \chi_i' \rangle \right] \tag{A1.3}$$

χ_i' is the molecular orbital χ_i, but including a spin factor α or β. The Slater Determinant S_k is an anti-symmetrized product of nine χ_i''s. $\langle \chi_i' | h_1 | \chi_j' \rangle$ means

$$\langle \chi_i' | h_1 | \chi_j' \rangle = \int \chi_i'^*(1) h_1^{(1)} \chi_j'(1) dv(1). \tag{A1.4}$$

The integration in (A1.4) includes an integral over spin as well as space. $\langle \chi_i', \chi_j' | h_2 | \chi_k', \chi_l' \rangle$ is defined by

$$\langle \chi_i', \chi_j' | h_2 | \chi_k', \chi_l' \rangle = \int\int \chi_i'^*(1) \chi_j'^*(2) \, h_2^{(1,2)} \chi_k'(1) \chi_l'(2) \times dv(1) dv(2). \tag{A1.5}$$

The integration in (A1.5) is over spins as well as space. The volume element dv(i) in (A1.4) and (A1.5) is $r_i^2 dr_i \sin\theta_i \, d\theta_i \, d\varphi_i$.

If $S_k \neq S_l$, permute the molecular orbitals with spin, χ'_i, in S_k and S_l so that there is the maximum possible coincidence between the two. If, after this permutation, the two Slater Determinants differ only in that S_k has χ'_a in the position where S_l has χ'_c, then

$$\int S_k^* \, h_0 \, S_l dV = 0, \tag{A1.6}$$

$$\int S_k^* \left(\sum_i h_1^{(i)} \right) S_l dV = \pm \langle \chi'_a | h_1 | \chi'_c \rangle \ , \tag{A1.7}$$

and

$$\int S_k^* \left(\tfrac{1}{2} \sum_{i \neq j} h_2^{(i,j)} \right) S_l dV = \pm \sum_i \left[\langle \chi'_a \chi'_i | h_2 | \chi'_c \chi'_i \rangle - \langle \chi'_a \chi'_i | h_2 | \chi'_i \chi'_c \rangle \right]. \tag{A1.8}$$

The + (-) sign in (A1.7) and (A1.8) is to be taken if an even (odd) number of permutations are required to bring S_k and S_l into maximum coincidence.

If, after the permutation, S_k and S_l differ in two positions, χ'_a and χ'_b for S_k, and correspondingly χ'_c and χ'_d for S_l, then

$$\int S_k^* \, h_0 \, S_l dV = 0, \tag{A1.9}$$

$$\int S_k^* \left(\sum_i h_1^{(i)} \right) S_l dV = 0, \tag{A1.10}$$

and

$$\int S_k^*\left(\tfrac{1}{2}\sum_{i\neq j} h_2^{(i,j)}\right)S_l\,dV = \pm\left[\langle \chi_a'\chi_b' | h_2 | \chi_c'\chi_d'\rangle - \langle \chi_a'\chi_b' | h_2 | \chi_d'\chi_c'\rangle\right]. \qquad \text{(A1.11)}$$

The interpretation of the $\pm$ sign in (A1.11) is the same as in (A1.7) and (A1.8).

If S_k and S_l differ by more than two χ_i', then the matrix elements of H between them vanish.

The integrations over spin in (A1.1) to (A1.11) are easily done. For example, in an obvious notation,

$$\langle \chi_i', \chi_j' | h_2 | \chi_k', \chi_l'\rangle = \delta_{s_i,s_k}\,\delta_{s_j,s_l}\langle \chi_i, \chi_j | h_2 | \chi_k, \chi_l\rangle . \qquad \text{(A1.12)}$$

APPENDIX 2

INTEGRALS OVER SLATER-TYPE ORBITALS

The simplest case is an overlap integral

$$\langle \phi_1 | \phi_2 \rangle = \delta_{\ell_1,\ell_2}\, \delta_{m_1,m_2}\, A(n_1, \xi_1) A(n_2, \xi_2) / A^2(\bar{n}, \bar{\xi}). \tag{A2.1}$$

In (A2.1), the Slater-type orbital ϕ_i is specified by n_i, ℓ_i, m_i and ξ_i. (See (4.1) and (4.3)). $\bar{\xi}$, $\bar{n}$, and $A(n, \xi)$ are defined by

$$\bar{\xi} = \tfrac{1}{2}(\xi_1 + \xi_2), \tag{A2.2}$$

$$\bar{n} = \tfrac{1}{2}(n_1 + n_2), \tag{A2.3}$$

and

$$A(n, \xi) = \sqrt{\frac{(2\xi)^{2n+1}}{(2n)!}}\ . \tag{A2.4}$$

The three one-electron integrals are the kinetic energy integral,

$$\langle \phi_1 | -\tfrac{1}{2}\nabla^2 | \phi_2 \rangle = -\frac{\langle \phi_1 | \phi_2 \rangle}{4\bar{n}(2\bar{n} - 1)} \times$$

$$\left[\xi_2^2 n_1(n_1-1) - 2\xi_1\xi_2 n_1 n_2 + \xi_1^2 n_2(n_2-1) - \ell_1(\ell_1+1)(2\bar{\xi})^2\right], \tag{A2.5}$$

the oxygen attraction integral,

$$\langle \phi_1 | -8/r | \phi_2 \rangle = -8\delta_{\ell_1,\ell_2}\, \delta_{m_1,m_2}\, \frac{A(n_1, \xi_1) A(n_2, \xi_2)}{A^2(\bar{n} - \tfrac{1}{2}, \bar{\xi})}, \tag{A2.6}$$

and the hydrogen attraction integral,

$$\langle \phi_1 | \frac{-1}{|\vec{r} - \vec{R}_1|} | \phi_2 \rangle = -\delta_{m_1,m_2} \frac{A(n_1,\xi_1)A(n_2,\xi_2)}{(2\bar{\xi})^{2\bar{n}}}$$

$$\times \sum_{k=0,2,\ldots}^{\infty} C^k(\ell_1,m_1;\ell_2,m_2)\left[(\bar{\rho})^{-(k+1)} \gamma(2\bar{n}+k+1,\bar{\rho}) + (\bar{\rho})^{k} \Gamma(2\bar{n}-k,\bar{\rho}) \right] . \quad (A2.7)$$

The C^k in (A2.7) are Condon-Shortley coefficients (Condon and Shortley, 1951). $\bar{\rho}$, γ and Γ are defined by

$$\bar{\rho} = \bar{\xi} R , \quad (A2.8)$$

$$\gamma(a,x) = \int_0^x e^{-t} t^{a-1} dt , \quad (A2.9)$$

and

$$\Gamma(a,x) = \int_x^{\infty} e^{-t} t^{a-1} dt . \quad (A2.10)$$

The one-centre two-electron integral is given by

$$\langle \phi_1, \phi_2 | h_2 | \phi_3, \phi_4 \rangle = \delta_{m_1-m_3,m_4-m_2} \times$$

$$A(n_1,\xi_1)A(n_2,\xi_2)A(n_3,\xi_3)A(n_4,\xi_4) \times$$

$$\sum_{k=0}^{\infty} C^k(\ell_1,m_1;\ell_3,m_3)C^k(\ell_4,m_4;\ell_2,m_2) \times$$

$$\left\{ \left[A(\bar{n}_1-\tfrac{1}{2}k-\tfrac{1}{2},\bar{\xi}_1)A(\bar{n}_2+\tfrac{1}{2}k,\bar{\xi}_2)\right]^{-2} I_{1-\eta}(2\bar{n}_2+k+1,2\bar{n}_1-k) \right.$$

$$\left. + \left[A(\bar{n}_2-\tfrac{1}{2}k-\tfrac{1}{2},\bar{\xi}_2)A(\bar{n}_1+\tfrac{1}{2}k,\bar{\xi}_1)\right]^{-2} I_{\eta}(2\bar{n}_1+k+1,2\bar{n}_2-k) \right\}, \quad (A2.11)$$

where

$$\bar{\xi}_1 = \tfrac{1}{2}(\xi_1+\xi_3), \tag{A2.12}$$

$$\bar{\xi}_2 = \tfrac{1}{2}(\xi_2+\xi_4), \tag{A2.13}$$

$$\eta = \bar{\xi}_1/(\bar{\xi}_1+\bar{\xi}_2), \tag{A2.14}$$

$$\bar{n}_1 = \tfrac{1}{2}(n_1+n_3), \tag{A2.15}$$

$$\bar{n}_2 = \tfrac{1}{2}(n_2+n_4), \tag{A2.16}$$

and $I_x(p,q)$ is the Incomplete Beta function

$$I_x(p,q) = \frac{\int_0^x t^{p-1}\,(1-t)^{q-1}dt}{\int_0^1 t^{p-1}\,(1-t)^{q-1}dt} \quad . \tag{A2.17}$$

APPENDIX 3

COMMENTS ON A PROCEDURE USED IN THE $^2\Sigma^-$ CALCULATION

The potential energy curve and corresponding wavefunction for the second lowest $^2\Sigma^-$ state were calculated by minimizing the second lowest eigenvalue of the Hamiltonian matrix. This procedure can produce erroneous results. The true wavefunction for this state is orthogonal to the true wavefunction for the lowest $^2\Sigma^-$ state. The trial wavefunction for the upper state should therefore be constrained to be orthogonal to the true wavefunction for the lowest state. Since the latter is not known, this constraint cannot be exactly realized.

However, the calculated upper state wavefunction is orthogonal to an approximate wavefunction for the lowest state, since they are non-degenerate eigenvectors of the same Hamiltonian matrix. If the latter wavefunction is a good approximation to the true wavefunction, the procedure can be expected to produce reasonable results.

The accuracy of this approximate wavefunction has not been checked. There is, however, reason to expect it to be fair. The lowest state wavefunction depends to a large degree on the parameters for only the 1s, 2s, 2p, $(1s)_H$, and $(2p)_H$ atomic orbitals (see Figure 8.11). Of these parameters, only those for the 2p and $(1s)_H$ orbitals

were varied in the second lowest $^2\Sigma^-$ calculation. The differences between the parameters calculated in this manner and those calculated by minimizing the lowest eigenvalue, while not insignificant, are not great (see Figures 8.3 and 8.7). It is quite probable, then, that the results obtained by minimizing the second lowest eigenvalue are not wildly inaccurate.